Design FPGA-Based Chattering-free Sliding Mode Controller for PUMA Robot Manipulator

Mahsa Piltan[1], Abdolwahab Kazerouni[2] and Ali Rafie[3]

Department of Electronics, Kazeroun Branch, Islamic Azad University, Fars, Iran
[1]*mahsa.piltan@gmail.com,* [2] *a.w.kazerouni@gmail.com,*
[3]*Alirafiee_2000@yahoo.com*

Abstract

Design of a robust controller for multi input-multi output (MIMO) nonlinear uncertain dynamical system can be a challenging work. This research focuses on the design and analysis of a high performance chattering free PD plus PD partly sliding mode controller in presence of uncertainties. In this research, sliding mode controller is a robust and stable nonlinear controller, which selected to control of robot manipulator. The proposed approach effectively combines of design methods from switching sliding mode controller, and linear Proportional-Derivative (PD) control to improve the performance, stability and robustness of the sliding mode controller. To reduce the chattering with respect to stability and robustness; linear controller is added to the switching part of the sliding mode controller. The linear controller is to reduce the role of sliding surface slope and switching (sign) function. To improve the flexibility, design high speed and low cost controller, micro-electronic device (FPGA-Based) controller is introduced in this research. The proposed design is 30-bits FPGA-based controller for inputs and 35-bits for output. All joints of robot are used to test the controller in simulation environments, using VHDL code for the purpose of simulation in Xilinx. The maximum frequency in FPGA-based design is about 63.6 MHz and the delay time in this design is about 15.7 ns. It is observed that this controller is able to make as a fast response at 15.716 ns clock period with 63.6 MHZ of a maximum frequency and 4.407 ns for minimum input arrival time after clock. From investigation and synthesis summary, 30.286 ns for maximum input arrival time after clock with 33.018 MHZ frequencies, this design has 15.716 ns delays for each controller to 46 logic elements and the offset before CLOCK is 55.773 ns for 132 logic gates.

Keywords: *real-time operation, Field Programmable Gate Array (FPGA), improved partly sliding mode control, PUMA robot manipulator, VHDL, Xilinx, sampling time*

1. Introduction

Design a FPGA-based robust controller for multi input-multi output (MIMO) nonlinear uncertain dynamical system (*e.g.,* robot manipulator) is the main challenging work in this research. Robot manipulators are set of links which connected by joints, they are multi input and multi output (MIMO), nonlinear, time variant, uncertain dynamic systems and are developed either to replace human work in many fields such as in industrial or in the manufacturing. Complexities of the tasks caused to design mechanical architectures and robot manipulator with nonlinear behavior. These factors are:

- Time-varying parameters based on tear and ware.
- Simplifying suppositions in system modelling caused to have un-modelled dynamic parameters.
- External disturbance and noise measurement, which it is caused to generate uncertainties.

According to above discussion, robot manipulators are nonlinear uncertain systems with human-like behavior therefore, control of these systems are complicated. Robot manipulators are divided into two main groups, serial links robot manipulators and parallel links robot manipulators. PUMA robot manipulator is a serial link robot manipulator, in this type of robot links and joints are serially connected between base and end-effector. Study of robot manipulators are classified into two main subjects: kinematics and dynamics. Study of kinematics is important to design controller in practical applications. Dynamic modeling of robot manipulator is used to illustrate the behavior of robot manipulator (*e.g.,* MIMO, nonlinear, uncertain parameters and …), design of nonlinear conventional controller and for simulation. It also used to explain some dynamic parameters effect to system behavior. According to the literature [1] PUMA robot manipulator is a serial links, six degrees of freedom and highly nonlinear dynamic systems, which control of this system with linear behavior is the main challenge in this research.

To control of PUMA robot manipulator, three purposes are very important:

- **Stability**: Stability is due to the proper functioning of the system. A system is called stable if for any bounded input signal the system's output will stay bounded. Therefore, limitation of output deviation is very important for any design.
- **Robust**: Robust method is caused to achieve robust and stable performance in the presence of uncertainty and external disturbance. A system is robust when it would also work well under different conditions and external disturbance.
- **Reliability:** to control of nonlinear and uncertain systems, reliability play important role and most of model-base controller are reliable.

As a result, design a controller based on these three factors are the main challenge in this work. Based on control theory; controllers for robot manipulators are divided into two main collections:

Conventional control theory and intelligent control theory where, conventional control theories are work based on nonlinear dynamic parameters of robot manipulator and these are divided into two main categories: Linear control method and nonlinear control method. Intelligent control theory is worked based on intelligent control theory and it is free of nonlinear dynamic parameters of robot manipulator.

According to the dynamic formulation of robot manipulators, they are uncertain and there exist strong coupling effects between joints. The problem of coupling effects play important role to get best performance in robot manipulator. In linear controller this challenge can be reduced, with the following two methods:

- Limiting the performance of the system according to the required velocities and accelerations, but now the applications demand for faster and lighter robot manipulators.
- Using a high gear ratio (*e.g.,* 250 to 1) at the mechanical design step, in this method the price paid is increased due to the gears.

Therefore linear type of controller, such as PD, PI or PID controllers cannot be having a good results and performance.

To eliminate the above challenge and the computation burden as well as have stability, efficiency and robust controller, sliding mode controller is introduced in this part. This controller works very well in certain and partly uncertain condition [1, 10-11]. This controller has two important subparts, switching part and equivalent part. Switching part of controller is used to design suitable tracking performance based on very fast switching. This part has essential role to have a good trajectory performance in all joints. However this part is very important in uncertain condition but it is caused to chattering phenomenon in system performance. Chattering phenomenon can cause some important

mechanical problems [10]. However partly sliding mode controller is a robust and stable controller but there has chattering phenomenon [7-9]. Due to literature to reduce or eliminate the chattering two main methodologies are introduced [4-6]:

- Linear (saturation) boundary layer method
- Nonlinear artificial intelligence based method

However eliminating the *switching discountinous* function in sliding mode controllers are used in many research but it can causes to lost the robustness of control and accuracy. In this research reduce or eliminate the chattering according to maintain the robustness is the main objective. Switching function is caused to chattering but it is one of the main parts to design robust and high speed sliding mode controller. In sliding mode controller, sliding surface slope (λ) is the second factor to control the chattering, as a result the main task in the first objective is reduce or eliminate the chattering in sliding mode controller based on design parallel linear control methodology and discontinuous part. Sliding mode controller and linear control methodologies are robust based on Lyapunov theory, therefore; Lyapunov stability is proved in proposed chattering free sliding mode controller based on switching theory. To have high implementation speed, small size device and high speed processing, FPGA is introduced to design FPGA-based sliding mode controller because FPGA has parallel architecture. FPGAs Xilinx Spartan 3E families are one of the most powerful flexible Hardware Language Description (HDL) programmable IC's. To have the high speed processing FPGA based sliding mode controller in Xilinx ISE 9.1 is designed and implemented [13-15].

This paper is organized as follows; Section 2, has served as an introduction to the system dynamics and kinematics. Part 3, introduces and describes the methodology based on FPGA. Section 4 presents the simulation results and discussion of this algorithm applied to a robot manipulator and the final Section is describing the conclusion.

2. Theory

A robot is a machine which can be programmed to do a range of tasks. They have five fundamental components; brain, body, actuator, sensors and power source supply. A brain controls the robot's actions to best response to desired and actual inputs. A robot body is physical chasses which can use to holds all parts together. Actuators permit the robot to move based on electrical part (*e.g.,* motors) and mechanical part (*e.g.,* hydraulic piston). Sensors give robot information about its internal and external part of robot environment and power source supply is used to supply all parts of robot. Robot is divided into three main groups: robot manipulator, mobile robot and hybrid robot.

Robot manipulator is a collection of links which connect to each other by joints. Each joint provides one or more Degrees Of Freedom (DOF). Figure 1 shows robot manipulator part. The fixed link in this system is called the base, while the last link whose motion is prescribed and used to interact with the environment is called the end-effector [1]. Robot manipulator is divided into two main groups, serial links robot manipulator and parallel links robot manipulators.
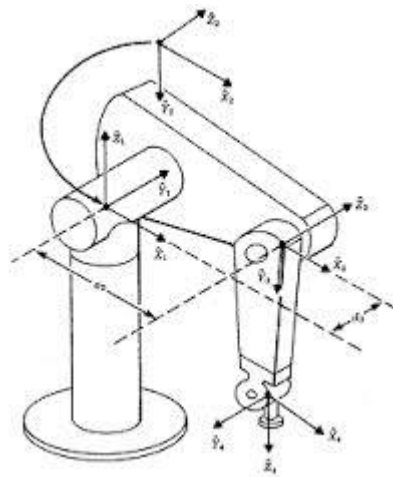
Figure 1. Robot Manipulator

Study of robot manipulators is classified into two main subjects: kinematics and dynamics. The study between rigid bodies and end-effector without any forces is called Robot manipulator Kinematics. Study of this part is very important to design controller and in practical applications. The study of motion without regard to the forces (manipulator kinematics) is divided into two main subjects: forward and inverse kinematics. Forward kinematics is a transformation matrix to calculate the relationship between position and orientation (pose) of task (end-effector) frame and joint variables. This part is very important to calculate the position and/or orientation error to calculate the controller's qualify. Forward kinematics matrix is a 4×4 matrix which 9 cells are show the orientation of end-effector, 3 cells show the position of end-effector and 4 cells are fix scaling factor. Inverse kinematics is a type of transformation functions that can used to find possible joints variable (displacements and/or angles) when all position and orientation (pose) of task be clear [2]. Figure 2 shows the application of forward and inverse kinematics.
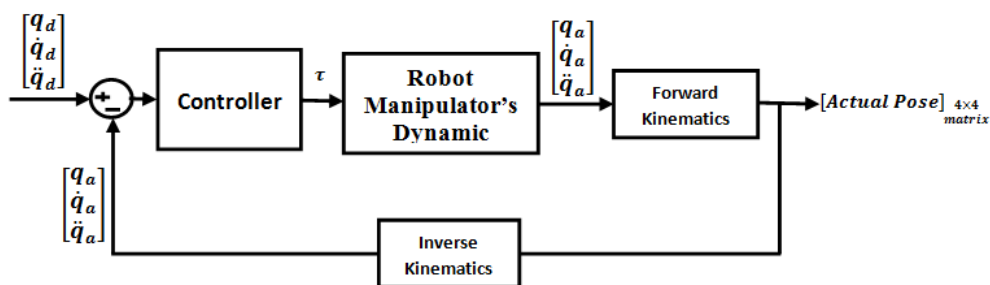

Figure 2. The Application of FORWARD and Inverse Kinematics

In this research to forward kinematics is used to system modeling. Wu has proposed PUMA 560 robot arm forward kinematics based on accurate analysis [4]. The main target in forward kinematics is calculating the following function:

$$\Psi(X, q) = 0 \tag{1}$$

Where $\Psi(.) \in R^n$ is a nonlinear vector function, $X = [X_1, X_2, \ldots \ldots, X_l]^T$ is the vector of task space variables which generally endeffector has six task space variables, three position and three orientation, $q = [q_1, q_2, \ldots, q_n]^T$ is a vector of angles or displacement, and finally n is the number of actuated joints.

Calculate robot manipulator forward kinematics is divided into four steps as follows;

- Link descriptions
- Denavit-Hartenberg (D-H) convention table
- Frame attachment
- Forward kinematics

The first step to analyze forward kinematics is link descriptions. This item must to describe and analyze four link and joint parameters. The link description parameters are; link length (a_i), twist angle (α_i), link offset (d_i) and joint angle (θ_i). Where link twist, is the angle between Z_i and Z_{i+1} about an X_i, link length, is the distance between Z_i and Z_{i+1} along X_i and d_i, offset, is the distance between X_{i-1} and X_i along Z_i axis. In these four parameters three of them are fixed and one of parameters is variable. If system has rotational joint, joint angle (θ_i) is variable and if it has prismatic joint, link offset (d_i) is variable.

The second step to compute Forward Kinematics (F.K) of robot manipulator is finding the standard D-H parameters. The Denavit-Hartenberg (D-H) convention is a method of drawing robot manipulators free body diagrams. Denvit-Hartenberg (D-H) convention study is compulsory to calculate forward kinematics in robot manipulator. Table 1 shows the standard D-H parameters for N-DOF robot manipulator. Figure 3 shows the D-H notation of research's plan (PUMA robot manipulator).

Table 1. The Denavit Hartenberg Parameter

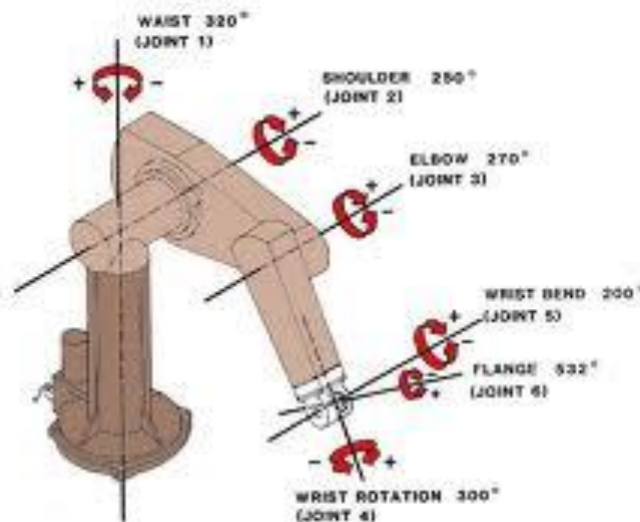| Link i	θ_i(rad)	α_i(rad)	a_i(m)	d_i(m)
1	θ_1	α_1	a_1	d_1
2	θ_2	α_2	a_2	d_2
3	θ_3	α_3	a_3	d_3
....	....	....	....	....
....	....	....	....	....
N	θ_n	n	a_5	d_n

Figure 3. D-H notation PUMA Robot Manipulator [5]

The third step to compute Forward kinematics for robot manipulator is finding the frame attachment matrix. The rotation matrix from $\{F_i\}$ to $\{F_{i-1}\}$ is given by the following equation;

$$R_i^{i-1} = U_{i(\theta_i)}V_{i(\alpha_i)} \tag{2}$$

Where $U_{i(\theta_i)}$ is given by the following equation [2];

$$U_{i(\theta_i)} = \begin{bmatrix} cos(\theta_i) & -sin(\theta_i) & 0 \\ sin(\theta_i) & cos(\theta_i) & 0 \\ 0 & 0 & 1 \end{bmatrix} \tag{3}$$

and $V_{i(\alpha_i)}$ is given by the following equation [2];

$$V_{i(\theta_i)} = \begin{bmatrix} 1 & 0 & 0 \\ 0 & cos(\alpha_i) & -sin(\alpha_i) \\ 0 & sin(\alpha_i) & cos(\alpha_i) \end{bmatrix} \tag{4}$$

So (R_n^0) is given by [2]

$$R_n^0 = (U_1 V_1)(U_2 V_2) \ldots \ldots \ldots (U_n V_n) \tag{5}$$

$$_n^{n-1}T = \begin{bmatrix} R_n^{n-1} & d_n^{n-1} \\ 0 & 1 \end{bmatrix} \tag{6}$$

The transformation $_n^0T$ (frame attachment) matrix is compute as the following formulation;

$$_1^{i-1}T = \begin{bmatrix} C\theta_i & -S\theta_i & 0 & a_{i-1} \\ S\theta_i\,C\alpha_{i-1} & C\theta_i\,C\alpha_{i-1} & -S\alpha_{i-1} & -S\alpha_{i-1}d_i \\ S\theta_i\,S\alpha_{i-1} & C\theta_i\,S\alpha_{i-1} & C\alpha_{i-1} & C\alpha_{i-1}d_i \\ 0 & 0 & 0 & 1 \end{bmatrix} \tag{7}$$

The forth step is calculate the forward kinematics by the following formulation [2]

$$FK = {}_n^0T = {}_1^0T.{}_2^1T.{}_3^2T \ldots \ldots. {}_n^{n-1}T = \begin{bmatrix} R_n^0 & d_n^0 \\ 0 & 1 \end{bmatrix} \tag{8}$$

Based on above formulation the final formulation for PUMA robot manipulator is;

$$_6^0T = \begin{bmatrix} N_x & B_x & T_x & P_x \\ N_y & B_y & T_y & P_y \\ N_z & B_z & T_z & P_z \\ 0 & 0 & 0 & 1 \end{bmatrix} \tag{9}$$

Table 2 shows the PUMA Denavit-Hartenberg notations.

Table 2. PUMA D-H Notations [6]

Link i	θ_i(rad)	α_i(rad)	a_i(m)	d_i(m)
1	θ_1	$-\pi/2$	0	0
2	θ_2	0	0.4318	0.14909
3	θ_3	$\pi/2$	0.0203	0
4	θ_4	$-\pi/2$	0	0.43307
5	θ_5	$\pi/2$	0	0
6	θ_6	0	0	0.05625

Based on [6] and frame attachment matrix the position and orientation (pose) matrix compute as belows;

$$Nx = cos(\theta_6) \times (cos(\theta_5) \times (cos(\theta_4) \times cos(\theta_2 + \theta_3) \times cos(\theta_1) + sin(\theta_1) \times sin(\theta_1)) + sin(\theta_5) \times sin(\theta_2 + \theta_3) \times cos(\theta_1)) + sin(\theta_6) \times (sin(\theta_4) \times cos(\theta_2 + \theta_3) \times cos(\theta_1) - cos(\theta_4) \times sin(\theta_1)) \tag{10}$$

$$Ny = cos(\theta_6) \times (cos(\theta_5) \times (cos(\theta_4) \times cos(\theta_2 + \theta_3) \times sin(\theta_1) - sin(\theta_4) \times cos(\theta_1)) + sin(\theta_5) \times sin(\theta_2 + \theta_3) \times sin(\theta_1)) + sin(\theta_6) \times (sin(\theta_4) \times cos(\theta_2 + \theta_3) \times sin(\theta_1) + cos(\theta_4) \times cos(\theta_1)) \tag{11}$$

$$Nz = cos(\theta_6) \times (cos(\theta_5) \times cos(\theta_4) \times sin(\theta_2 + \theta_3) - sin(\theta_5) \times cos(\theta_2 + \theta_3)) + sin(\theta_6) \times sin(\theta_4) \times sin(\theta_2 + \theta_3) \tag{12}$$

$$Bx = -sin(\theta_6) \times (cos(\theta_5) \times (cos(\theta_4) \times cos(\theta_2 + \theta_3) \times cos(\theta_1) + sin(\theta_4) \times sin(\theta_1)) + sin(\theta_5) \times sin(\theta_2 + \theta_3) \times cos(\theta_1)) + cos(\theta_6) \times (sin(\theta_4) \times cos(\theta_2 + \theta_3) \times cos(\theta_1) - cos(\theta_4) \times sin(\theta_1)) \tag{13}$$

$$By = -sin(\theta_6) \times (cos(\theta_5) \times (cos(\theta_4) \times cos(\theta_2 + \theta_3) \times sin(\theta_1) - sin(\theta_4) \times cos(\theta_1)) + sin(\theta_5) \times sin(\theta_2 + \theta_3) \times sin(\theta_1)) + cos(\theta_6) \times (sin(\theta_4) \times cos(\theta_2 + \theta_3) \times sin(\theta_1) + cos(\theta_4) \times cos(\theta_1)) \tag{14}$$

$$Bz = -sin(\theta_6) \times (cos(\theta_5) \times cos(\theta_4) \times sin(\theta_2 + \theta_3) - sin(\theta_5) \times cos(\theta_2 + \theta_3)) + cos(\theta_6) \times sin(\theta_4) \times sin(\theta_2 + \theta_3) \tag{15}$$

$$Tx = sin(\theta_5) \times (cos(\theta_4) \times cos(\theta_2 + \theta_3) \times cos(\theta_1) + sin(\theta_4) \times sin(\theta_1)) - cos(\theta_5) \times sin(\theta_2 + \theta_3) \times cos(\theta_1) \tag{16}$$

$$Ty = sin(\theta_5) \times (cos(\theta_4) \times cos(\theta_2 + \theta_3) \times sin(\theta_1) - sin(\theta_4) \times cos(\theta_1)) - cos(\theta_5) \times sin(\theta_2 + \theta_3) \times sin(\theta_1) \tag{17}$$

$$Tz = sin(\theta_5) \times cos(\theta_4) \times sin(\theta_2 + \theta_3) + cos(\theta_5) \times cos(\theta_2 + \theta_3) \tag{18}$$

$$Px = 0.4331 \times sin(\theta_2 + \theta_3) \times cos(\theta_1) + 0.0203 \times cos(\theta_2 + \theta_3) \times cos(\theta_1) - 0.1491 \times sin(\theta_1) + 0.4318 \times cos(\theta_2 cos(\theta_1) \tag{19}$$

$$Py = 0.4331 \times sin(\theta_2 + \theta_3) \times sin(\theta_1) + 0.0203 \times cos(\theta_2 + \theta_3) \times sin(\theta_1) + 0.1491 \times cos(\theta_1) + 0.4312 \times cos(\theta_2) \times sin(\theta_1) \tag{20}$$

$$Pz = -0.4331 \times cos(\theta_2 + \theta_3) + 0.0203 \times sin(\theta_2 + \theta_3) + 0.4318 \times sin(\theta_2) \tag{21}$$

A dynamic function is the study of motion with regard to the forces. Dynamic modeling of robot manipulators is used to illustrate the behavior of robot manipulator (*e.g.,* nonlinear dynamic behavior), design of nonlinear conventional controller and for simulation. It is used to analyses the relationship between dynamic functions output (*e.g.,* joint motion, velocity, and accelerations) to input source of dynamic functions (*e.g.,* force/torque or current/voltage). Dynamic functions is also used to explain the some dynamic parameter's effect (*e.g.,* inertial matrix, Coriolios, Centrifugal, and some other parameters) to system's behavior [2].

The equation of a multi degrees of freedom (DOF) robot manipulator is considered by the following equation[3]:

$$[A(q)]\ddot{q} + [N(q, \dot{q})] = [\tau] \tag{22}$$

Where τ is actuator's torque and is $n \times 1$ vector, A (q) is positive define inertia and is $n \times n$ symmetric matrix based on the following formulation;

$$A(q) = \begin{bmatrix} A_{11} & A_{12} & \dots & \dots & \dots & A_{1n} \\ A_{21} & \dots & \dots & \dots & \dots & A_{2n} \\ \dots & \dots & \dots & \dots & \dots & \dots \\ \dots & \dots & \dots & \dots & \dots & \dots \\ \dots & \dots & \dots & \dots & \dots & \dots \\ A_{n.1} & \dots & \dots & \dots & \dots & A_{n.n} \end{bmatrix} \qquad (23)$$

$N(q, \dot{q})$ is the vector of nonlinearity term, and q is $n \times 1$ joints variables. If all joints are revolute, the joint variables are angle (θ) and if these joints are translated, the joint variables are translating position (d). According to (22) the nonlinearity term of robot manipulator is derived as three main parts; Coriolis $b(q)$, Centrifugal $C(q)$, and Gravity $G(q)$. Consequently the robot manipulator dynamic equation can also be written as [1]:

$$[N(q, \dot{q})] = [V(q, \dot{q})] + [G(q)] \qquad (24)$$

$$[V(q, \dot{q})] = [b(q)][\dot{q}\,\dot{q}] + [C(q)][\dot{q}]^2 \qquad (25)$$

$$\tau = A(q)\ddot{q} + b(q)[\dot{q}\,\dot{q}] + C(q)[\dot{q}]^2 + G(q) \qquad (26)$$

Where,

$b(q)$ is a Coriolis torque matrix and is $n \times \frac{n \times (n-1)}{2}$ matrix, $C(q)$ is Centrifugal torque matrix and is $n \times n$ matrix, Gravity is the force of gravity and is $n \times 1$ matrix, $[\dot{q}\,\dot{q}]$ is vector of joint velocity that it can give by: $[\dot{q}_1.\dot{q}_2, \dot{q}_1.\dot{q}_3, \dots, \dot{q}_1.\dot{q}_n, \dot{q}_2.\dot{q}_3, \dots]^T$, and $[\dot{q}]^2$ is vector, that it can given by: $[\dot{q}_1{}^2, \dot{q}_2{}^2, \dot{q}_3{}^2, \dots]^T$. According to the basic information from university all functions are derived as the following form;

$$Outputs = function\ (inputs) \qquad (27)$$

In the dynamic formulation of robot manipulator the inputs are torques matrix and the outputs are actual joint variables, consequently (28) is derived as (27);

$$q = function\ (\tau) \qquad (28)$$

$$\ddot{q} = A^{-1}(q).\{\tau - N(q, \dot{q})\} \qquad (29)$$

$$q = \iint A^{-1}(q).\{\tau - N(q, \dot{q})\} \qquad (30)$$

The Coriolis matrix (b) is a $n \times \frac{n(n-1)}{2}$ matrix which calculated as follows;

$$b(q) = \begin{bmatrix} b_{112} & b_{113} & \dots & b_{11n} & b_{123} & \dots & b_{12n} & \dots & \dots & b_{1.n-1.n} \\ b_{212} & \dots & \dots & b_{21n} & b_{223} & \dots & \dots & \dots & \dots & b_{2.n-1.n} \\ \dots & \dots & \dots & \dots & \dots & \dots & \dots & \dots & \dots & \dots \\ \dots & \dots & \dots & \dots & \dots & \dots & \dots & \dots & \dots & \dots \\ \dots & \dots & \dots & \dots & \dots & \dots & \dots & \dots & \dots & \dots \\ b_{n.1.2} & \dots & \dots & b_{n.1.n} & \dots & \dots & \dots & \dots & \dots & b_{n.n-1.n} \end{bmatrix} \qquad (31)$$

The Centrifugal matrix (C) is a $n \times n$ matrix;

$$C(q) = \begin{bmatrix} C_{11} & \cdots & C_{1n} \\ \vdots & \ddots & \vdots \\ C_{n1} & \cdots & C_{nn} \end{bmatrix} \qquad (32)$$

The Gravity vector (G) is a $n \times 1$ vector;

$$G(q) = \begin{bmatrix} g_1 \\ g_2 \\ \vdots \\ g_n \end{bmatrix} \qquad (33)$$

According to [8-11], the dynamic formulations of six Degrees of Freedom serial links PUMA robot manipulator are computed by;

$$A(\ddot{\theta})\begin{bmatrix}\ddot{\theta}_1\\\ddot{\theta}_2\\\ddot{\theta}_3\\\ddot{\theta}_4\\\ddot{\theta}_5\\\ddot{\theta}_6\end{bmatrix} + B(\theta)\begin{bmatrix}\dot{\theta}_1\dot{\theta}_2\\\dot{\theta}_1\dot{\theta}_3\\\dot{\theta}_1\dot{\theta}_4\\\dot{\theta}_1\dot{\theta}_5\\\dot{\theta}_1\dot{\theta}_6\\\dot{\theta}_2\dot{\theta}_3\\\dot{\theta}_2\dot{\theta}_4\\\dot{\theta}_2\dot{\theta}_5\\\dot{\theta}_2\dot{\theta}_6\\\dot{\theta}_3\dot{\theta}_4\\\dot{\theta}_3\dot{\theta}_5\\\dot{\theta}_3\dot{\theta}_6\\\dot{\theta}_4\dot{\theta}_5\\\dot{\theta}_4\dot{\theta}_6\\\dot{\theta}_5\dot{\theta}_6\end{bmatrix} + C(\theta)\begin{bmatrix}\dot{\theta}_1^2\\\dot{\theta}_2^2\\\dot{\theta}_3^2\\\dot{\theta}_4^2\\\dot{\theta}_5^2\\\dot{\theta}_6^2\end{bmatrix} + G(\theta) = \begin{bmatrix}\tau_1\\\tau_2\\\tau_3\\\tau_4\\\tau_5\\\tau_6\end{bmatrix} \tag{34}$$

Where

$$A(q) = \begin{bmatrix}A_{11} & A_{12} & A_{13} & 0 & 0 & 0\\A_{21} & A_{22} & A_{23} & 0 & 0 & 0\\A_{31} & A_{32} & A_{33} & 0 & A_{35} & 0\\0 & 0 & 0 & A_{44} & 0 & 0\\0 & 0 & 0 & 0 & A_{55} & 0\\0 & 0 & 0 & 0 & 0 & A_{66}\end{bmatrix} \tag{35}$$

According to [1] the inertial matrix elements (A) are

$A_{11} = I_{m1} + I_1 + I_3 \times \cos(\theta_2)\cos(\theta_2) + I_7\sin(\theta_2 + \theta_3)\sin(\theta_2 + \theta_3) + I_{10}\sin(\theta_2 + \theta_3)\cos(\theta_2 + \theta_3) + I_{11}\sin(\theta_2)\cos(\theta_2) + I_{21}\sin(\theta_2 + \theta_3)\sin(\theta_2 + \theta_3) + 2 + [I_5\cos(\theta_2)\sin(\theta_2 + \theta_3) + I_{12}\cos(\theta_2)\cos(\theta_2 + \theta_3) + I_{15}\sin(\theta_2 + \theta_3)\sin(\theta_2 + \theta_3) + I_{16}\cos(\theta_2)\sin(\theta_2 + \theta_3) + I_{22}\sin(\theta_2 + \theta_3)\cos(\theta_2 + \theta_3)$ (36)

$A_{12} = I_4\sin(\theta_2) + I_8\cos(\theta_2 + \theta_3) + I_9\cos(\theta_2) + I_{13}\sin(\theta_2 + \theta_3) - I_{18}\cos(\theta_2 + \theta_3)$ (37)

$A_{13} = I_8\cos(\theta_2 + \theta_3) + I_{13}\sin(\theta_2 + \theta_3) - I_{18}\cos(\theta_2 + \theta_3)$ (38)

$A_{22} = I_{m2} + I_2 + I_6 + 2[I_5\sin(\theta_3) + I_{12}\cos(\theta_2) + I_{15} + I_{16}\sin(\theta_3)]$ (39)

$A_{23} = I_5\sin(\theta_3) + I_6 + I_{12}\cos(\theta_3) + I_{16}\sin(\theta_3) + 2I_{15}$ (40)

$A_{33} = I_{m3} + I_6 + 2I_{15}$ (41)

$A_{35} = I_{15} + I_{17}$ (42)

$A_{44} = I_{m4} + I_{14}$ (43)

$A_{55} = I_{m5} + I_{17}$ (44)

$A_{66} = I_{m6} + I_{23}$ (45)

$A_{21} = A_{12}, A_{31} = A_{13} \; and \; A_{32} = A_{23}$ (46)

Based on [1] the Corilios (b) matrix elements are;

$$b(q) = \begin{bmatrix} b_{112} & b_{113} & 0 & b_{115} & 0 & b_{123} & 0 & 0 & 0 & 0 & 0 & 0 & 0 & 0 & 0 \\ 0 & 0 & b_{214} & 0 & 0 & b_{223} & 0 & b_{225} & 0 & 0 & b_{235} & 0 & 0 & 0 & 0 \\ 0 & 0 & b_{314} & 0 & 0 & 0 & 0 & 0 & 0 & 0 & 0 & 0 & 0 & 0 & 0 \\ b_{412} & b_{413} & 0 & b_{415} & 0 & 0 & 0 & 0 & 0 & 0 & 0 & 0 & 0 & 0 & 0 \\ 0 & 0 & b_{514} & 0 & 0 & 0 & 0 & 0 & 0 & 0 & 0 & 0 & 0 & 0 & 0 \\ 0 & 0 & 0 & 0 & 0 & 0 & 0 & 0 & 0 & 0 & 0 & 0 & 0 & 0 & 0 \end{bmatrix} \tag{47}$$

Where,

$$b_{112} = 2\left[-I_3\sin(\theta_2)\cos(\theta_2) + I_5\cos(\theta_2 + \theta_2 + \theta_3) + I_7\sin(\theta_2 + \theta_3)\cos(\theta_2 + \theta_3) - I_{12}\sin(\theta_2 + \theta_2 + \theta_3) - I_{15}2\sin(\theta_2 + \theta_3)\cos(\theta_2 + \theta_3) + I_{16}\cos(\theta_2 + \theta_2 + \theta_3) + I_{21}\sin(\theta_2 + \theta_3)\cos(\theta_2 + \theta_3) + I_{22}\left(1 - 2\sin(\theta_2 + \theta_3)\sin(\theta_2 + \theta_3)\right)\right] + I_{10}\left(1 - 2\sin(\theta_2 + \theta_3)\sin(\theta_2 + \theta_3)\right) + I_{11}\left(1 - 2\sin(\theta_2)\sin(\theta_2)\right) \tag{48}$$

$$b_{113} = 2\left[I_5\cos(\theta_2)\cos(\theta_2 + \theta_3) + I_7\sin(\theta_2 + \theta_3)\cos(\theta_2 + \theta_3) - I_{12}\cos(\theta_2)\sin(\theta_2 + \theta_2) + I_{15}2\sin(\theta_2 + \theta_3)\cos(\theta_2 + \theta_3) + I_{16}\cos(\theta_2)\cos(\theta_2 + \theta_3) + I_{21}\sin(\theta_2 + \theta_3)\cos(\theta_2 + \theta_3) + I_{22}\left(1 - 2\sin(\theta_2 + \theta_3)\sin(\theta_2 + \theta_3)\right)\right] + I_{10}\left(1 - 2\sin(\theta_2 + \theta_3)\sin(\theta_2 + \theta_3)\right) \tag{49}$$

$$b_{115} = 2[-\sin(\theta_2 + \theta_3)\cos(\theta_2 + \theta_3) + I_{15}2\sin(\theta_2 + \theta_3)\cos(\theta_2 + \theta_3) + I_{16}\cos(\theta_2)\cos(\theta_2 + \theta_3) + I_{22}\cos(\theta_2 + \theta_3)\cos(\theta_2 + \theta_3)] \tag{50}$$

$$b_{123} = 2[-I_8\sin(\theta_2 + \theta_3) + I_{13}\cos(\theta_2 + \theta_3) + I_{18}\sin(\theta_2 + \theta_3)] \tag{51}$$

$$b_{214} = I_{14}\sin(\theta_2 + \theta_3) + I_{19}\sin(\theta_2 + \theta_3) + 2I_{20}\sin(\theta_2 + \theta_3)(1 - 0.5) \tag{52}$$

$$b_{223} = 2[-I_{12}\sin(\theta_3) + I_5\cos(\theta_3) + I_{16}\cos(\theta_3)] \tag{53}$$

$$b_{235} = 2[I_{16}\cos(\theta_3) + I_{22}] \tag{54}$$

$$b_{314} = 2[I_{20}\sin(\theta_2 + \theta_3)(1 - 0.5)] + I_{14}\sin(\theta_2 + \theta_3) + I_{19}\sin(\theta_2 + \theta_3) \tag{55}$$

$$b_{412} = b_{214} = -[I_{14}\sin(\theta_2 + \theta_3) + I_{19}\sin(\theta_2 + \theta_3) + 2I_{20}\sin(\theta_2 + \theta_3)(1 - 0.5)] \tag{56}$$

$$b_{413} = -b_{314} = -2[I_{20}\sin(\theta_2 + \theta_3)(1 - 0.5)] + I_{14}\sin(\theta_2 + \theta_3) + I_{19}\sin(\theta_2 + \theta_3) \tag{57}$$

$$b_{415} = -I_{20}\sin(\theta_2 + \theta_3) - I_{17}\sin(\theta_2 + \theta_3) \tag{58}$$

$$b_{514} = -b_{415} = I_{20}\sin(\theta_2 + \theta_3) + I_{17}\sin(\theta_2 + \theta_3) \tag{59}$$

Based on above discussion $[b(q)]$ is 6×15 matrix and $[\dot{q}\dot{q}]$ is 15×1, therefore $[b(q).\dot{q}\dot{q}]$ is 6×1.

$$[b(q).\dot{q}\dot{q}]_{6\times1} = \begin{bmatrix} b_{112}.\dot{q}_1\dot{q}_2 + b_{113}.\dot{q}_1\dot{q}_3 + 0 + b_{115}.\dot{q}_1\dot{q}_5 + b_{123}.\dot{q}_2\dot{q}_3 \\ 0 + b_{214}.\dot{q}_1\dot{q}_4 + b_{223}.\dot{q}_2\dot{q}_3 + b_{225}.\dot{q}_2\dot{q}_5 + b_{235}.\dot{q}_3\dot{q}_5 \\ b_{314}.\dot{q}_1\dot{q}_4 \\ b_{412}.\dot{q}_1\dot{q}_2 + b_{413}.\dot{q}_1\dot{q}_3 + b_{415}.\dot{q}_1\dot{q}_5 \\ b_{514}.\dot{q}_1\dot{q}_4 \\ 0 \end{bmatrix} \tag{60}$$

According to [1] Centrifugal (C) matrix elements are;

$$C(q) = \begin{bmatrix} 0 & C_{12} & C_{13} & 0 & 0 & 0 \\ C_{21} & 0 & C_{23} & 0 & 0 & 0 \\ C_{31} & C_{32} & 0 & 0 & 0 & 0 \\ 0 & 0 & 0 & 0 & 0 & 0 \\ C_{51} & C_{52} & 0 & 0 & 0 & 0 \\ 0 & 0 & 0 & 0 & 0 & 0 \end{bmatrix} \tag{61}$$

Where,

$$c_{12} = I_4\cos(\theta_2) - I_8\sin(\theta_2 + \theta_3) - I_9\sin(\theta_2) + I_{13}\cos(\theta_2 + \theta_3) + I_{18}\sin(\theta_2 + \theta_3) \tag{62}$$

$$c_{13} = 0.5b_{123} = -I_8\sin(\theta_2 + \theta_3) + I_{13}\cos(\theta_2 + \theta_3) + I_{18}\sin(\theta_2 + \theta_3) \quad (63)$$

$$c_{21} = -0.5b_{112} = I_3\sin(\theta_2)\cos(\theta_2) - I_5\cos(\theta_2 + \theta_2 + \theta_3) - I_7\sin(\theta_2 + \theta_3)\cos(\theta_2 + \theta_3) + I_{12}\sin(\theta_2 + \theta_2 + \theta_3) + I_{15}2\sin(\theta_2 + \theta_3)\cos(\theta_2 + \theta_3) - I_{16}\cos(\theta_2 + \theta_2 + \theta_3) - I_{21}\sin(\theta_2 + \theta_3)\cos(\theta_2 + \theta_3) - I_{22}(1 - 2\sin(\theta_2 + \theta_3)\sin(\theta_2 + \theta_3)) - 0.5I_{10}(1 - 2\sin(\theta_2 + \theta_3)\sin(\theta_2 + \theta_3)) - 0.5I_{11}(1 - 2\sin(\theta_2)\sin(\theta_2)) \quad (64)$$

$$c_{22} = 0.5b_{223} = -I_{12}\sin(\theta_3) + I_5\cos(\theta_3) + I_{16}\cos(\theta_3) \quad (65)$$

$$c_{23} = -0.5b_{113} = -I_5\cos(\theta_2)\cos(\theta_2 + \theta_3) - I_7\sin(\theta_2 + \theta_3)\cos(\theta_2 + \theta_3) + I_{12}\cos(\theta_2)\sin(\theta_2 + \theta_2) - I_{15}2\sin(\theta_2 + \theta_3)\cos(\theta_2 + \theta_3) - I_{16}\cos(\theta_2)\cos(\theta_2 + \theta_3) - I_{21}\sin(\theta_2 + \theta_3)\cos(\theta_2 + \theta_3) - I_{22}(1 - 2\sin(\theta_2 + \theta_3)\sin(\theta_2 + \theta_3)) - 0.5I_{10}(1 - 2\sin(\theta_2 + \theta_3)\sin(\theta_2 + \theta_3)) \quad (66)$$

$$c_{31} = -c_{23} = I_{12}\sin(\theta_3) - I_5\cos(\theta_3) - I_{16}\cos(\theta_3) \quad (67)$$

$$c_{32} = -0.5b_{115} = \sin(\theta_2 + \theta_3)\cos(\theta_2 + \theta_3) - I_{15}2\sin(\theta_2 + \theta_3)\cos(\theta_2 + \theta_3) - I_{16}\cos(\theta_2)\cos(\theta_2 + \theta_3) - I_{22}\cos(\theta_2 + \theta_3)\cos(\theta_2 + \theta_3) \quad (68)$$

$$c_{52} = -0.5b_{225} = -I_{16}\cos(\theta_3) - I_{22} \quad (69)$$

$$[C(q).\dot{q}^2]_{6\times1} = \begin{bmatrix} c_{12}.q_2^2 + c_{13}.q_3^2 \\ c_{21}.q_1^2 + c_{23}.q_3^2 \\ c_{13}.q_1^2 + c_{32}.q_2^2 \\ 0 \\ c_{51}.q_1^2 + c_{52}.q_2^2 \\ 0 \end{bmatrix} \quad (70)$$

Gravity (G) Matrix elements are [1];

$$[G(q)]_{6\times1} = \begin{bmatrix} 0 \\ G_2 \\ G_3 \\ 0 \\ G_5 \\ 0 \end{bmatrix} \quad (71)$$

Where,

$$G_2 = g_1\cos(\theta_2) + g_2\sin(\theta_2 + \theta_3) + g_3\sin(\theta_2) + g_4\cos(\theta_2 + \theta_3) + g_5\sin(\theta_2 + \theta_3) \quad (72)$$

$$G_3 = g_2\sin(\theta_2 + \theta_3) + g_4\cos(\theta_2 + \theta_3) + g_5\sin(\theta_2 + \theta_3) \quad (73)$$

$$G_5 = g_5\sin(\theta_2 + \theta_3) \quad (74)$$

If $[I]_{6\times1} = [B]_{6\times1} + [C]_{6\times1} + [G]_{6\times1}$

Then $\ddot{q}$ is written as follows;

$$[\ddot{q}]_{6\times1} = [A^{-1}(q)]_{6\times6} \times \{[\tau]_{6\times1} - [I]_{6\times1}\} \quad (75)$$

K is presented as follows;

$$[K]_{6\times1} = \{[\tau]_{6\times1} - [I]_{6\times1}\} \quad (76)$$

$$[\ddot{q}]_{6\times1} = [A^{-1}(q)]_{6\times6} \times [K]_{6\times1} \quad (77)$$

$$[q]_{6\times1} = \iint [A^{-1}(q)]_{6\times6} \times [K]_{6\times1} \quad (78)$$

Basic information about inertial and gravitational constants is show in Tables 3 and 4 [8, 12].

Table 3. Inertial Constant Reference ($Kg.m^2$)

$I_1 = 1.43 \pm 0.05$	$I_2 = 1.75 \pm 0.07$
$I_3 = 1.38 \pm 0.05$	$I_4 = 0.69 \pm 0.02$
$I_5 = 0.372 \pm 0.031$	$I_6 = 0.333 \pm 0.016$
$I_7 = 0.298 \pm 0.029$	$I_8 = -0.134 \pm 0.014$
$I_9 = 0.0238 \pm 0.012$	$I_{10} = -0.0213 \pm 0.0022$
$I_{11} = -0.0142 \pm 0.0070$	$I_{12} = -0.011 \pm 0.0011$
$I_{13} = -0.00379 \pm 0.0009$	$I_{14} = 0.00164 \pm 0.000070$
$I_{15} = 0.00125 \pm 0.0003$	$I_{16} = 0.00124 \pm 0.0003$
$I_{17} = 0.000642 \pm 0.0003$	$I_{18} = 0.000431 \pm 0.00013$
$I_{19} = 0.0003 \pm 0.0014$	$I_{20} = -0.000202 \pm 0.0008$
$I_{21} = -0.0001 \pm 0.0006$	$I_{22} = -0.000058 \pm 0.000015$
$I_{23} = 0.00004 \pm 0.00002$	$I_{m1} = 1.14 \pm 0.27$
$I_{m2} = 4.71 \pm 0.54$	$I_{m3} = 0.827 \pm 0.093$
$I_{m4} = 0.2 \pm 0.016$	$I_{m5} = 0.179 \pm 0.014$
$I_{m6} = 0.193 \pm 0.016$	

Table 4. Gravitational Constant ($N.m$)

$g_1 = -37.2 \pm 0.5$	$g_2 = -8.44 \pm 0.20$
$g_3 = 1.02 \pm 0.50$	$g_4 = 0.249 \pm 0.025$
$g_5 = -0.0282 \pm 0.0056$	

3. Methodology: Design FPGA-Based Improved Partly Sliding Mode Controller

The main four objectives to design controllers are: stability, robust, minimum error and reliability. One of the robust nonlinear controllers which have been analyzed by many researchers especially in recent years to control of robot manipulator is sliding mode controller (SMC). Sliding mode controller (SMC) is robust conventional nonlinear controller in a partly uncertain dynamic system's parameters. This conventional nonlinear controller is used in several applications such as in robotics, process control, aerospace and power electronics. This controller can solve two most important challenging topics in control theory, stability and robustness [7-11]. The main idea to design sliding mode control is based on the following formulation;

$$\tau_{(q,t)} = \begin{cases} \tau_i^+(q,t) & if \ \ S_i > 0 \\ \tau_i^-(q,t) & if \ \ S_i < 0 \end{cases} \tag{79}$$

where S_i is sliding surface (switching surface), $i = 1, 2, \ldots \ldots, n$ for n-DOF robot manipulator, $\tau_i(q,t)$ is the ith torque of joint. According to above formulation the main

part of this control theory is switching part this idea is caused to increase the speed of response. Sliding mode controller is divided into two main sub parts:

- Discontinues controller(τ_{dis})
- Equivalent controller(τ_{eq})

Figure 4 shows the main part of sliding mode controller with application to serial links robot manipulator.
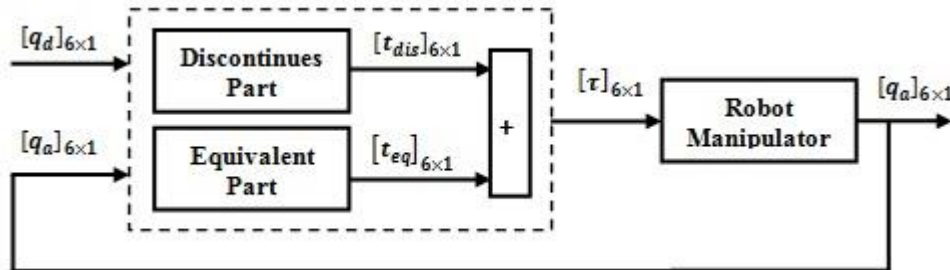

Figure 4. Block Diagram of Conventional Sliding Mode Controller

Discontinues controller is used to design suitable tracking performance based on very fast switching. This part of controller is work based on the linear type methodology; therefore it can be PD, PI and PID. Fast switching or discontinuous part have essential role to achieve to good trajectory following, but it is caused system instability and chattering phenomenon. Chattering phenomenon is one of the main challenges in conventional sliding mode controller and it can causes some important mechanical problems such as saturation and heats the mechanical parts of robot manipulators or drivers. Figure 5 shows the sliding surface and chattering phenomenon.
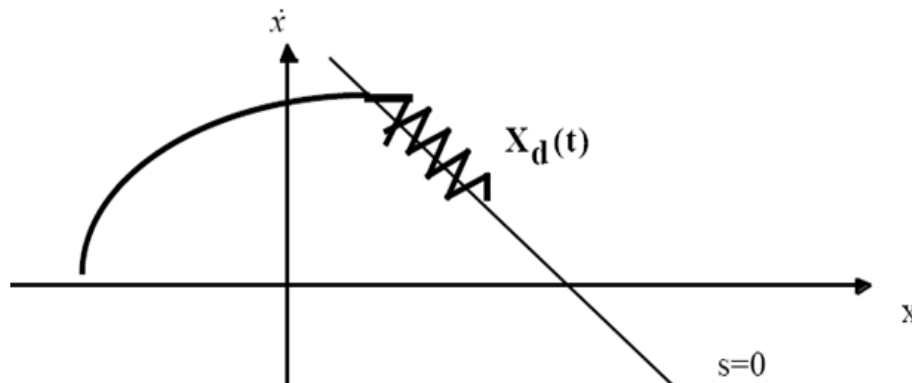

Figure 5. Sliding Surface and Chattering Phenomenon [2]

Equivalent part of robust nonlinear sliding mode controller is the impact of nonlinear term of serial links robot manipulator. It is caused to the control reliability and used to fine tuning the sliding surface slope [3, 7]. The equivalent part of sliding mode controller is the second challenge in uncertain systems especially in robot manipulator because in condition of uncertainty calculate the nonlinear term of robot manipulator's dynamic is very difficult or unfeasible. The formulations of sliding mode controller with application to six degrees of freedom serial links robot manipulator is presented based on [3, 7].

However, conventional sliding mode controller is used in many applications such as robot manipulator but, this controller has two main challenges [9]:

- chattering phenomenon
- nonlinear equivalent dynamic formulation in uncertain parameters

Based on the literature to reduce or eliminate the chattering, various papers have been reported by many researchers which classified into two main methods:

- boundary layer saturation method
- artificial intelligence based method

The boundary layer saturation method is used to reduce or eliminate the high frequency oscillation in conventional sliding mode controller. However this method can solve the challenge of chattering phenomenon but it has two main challenges; increase the error and reduces the speed of response.
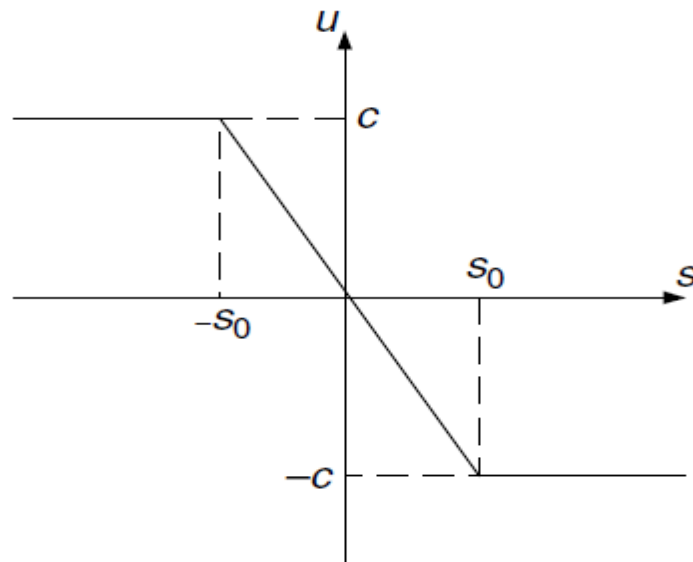

Figure 6. Linear Saturation Boundary Layer Functions [2]

To reduce the challenge of chattering as well as reduce the error Palm [4] design nonlinear intelligent saturation boundary layer function instead of linear saturation boundary method. According to Palm [4] design, the fuzzy controller has been had two inputs, seven linguistic variables and has 49 rule bases. This method can solve the challenge of chattering as well as error but design this type of controller is difficult and tune the fuzzy logic gain updating factors are very the main challenges in this theory. Figure 7 shows the nonlinear artificial intelligence sliding mode controller based on fuzzy logic methodology.
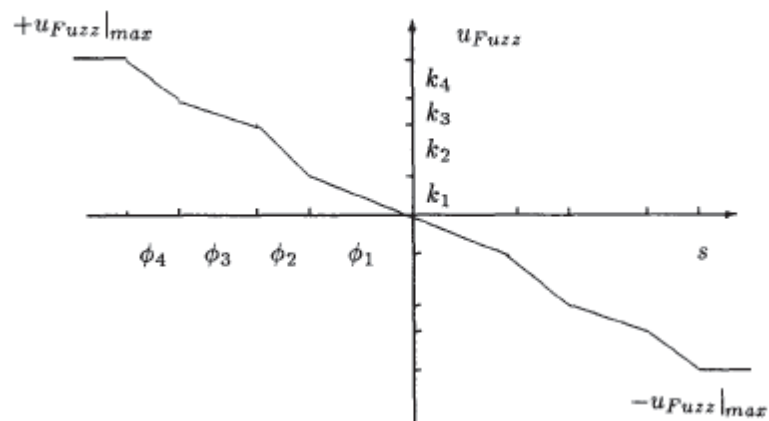

Figure 7. Nonlinear Fuzzy Saturation Boundary Layer Functions [4]

The main idea to design sliding mode control is based on the following formulation;

$$\tau_{(q,t)} = \begin{cases} \tau_i^+(q,t) & if \ S_i > 0 \\ \tau_i^-(q,t) & if \ S_i < 0 \end{cases} \tag{80}$$

where S_i is sliding surface (switching surface), $i = 1, 2, \ldots \ldots, n$ for n-DOF robot manipulator, $\tau_i(q,t)$ is the ith torque of joint. The dynamic formulation of nonlinear single input system is defined by [3]:

$$x^{(n)} = f(\vec{x}) + b(\vec{x})u \tag{81}$$

u is the vector of control input, $x^{(n)}$ is the nth derivation of x, $x = [x, \dot{x}, \ddot{x}, \ldots, x^{(n-1)}]^T$ is the state vector, $f(x)$ is unknown or uncertainty, and $b(x)$ is known *switching (SIGN)* function. The main target to design sliding mode controller is high speed train and high tracking accuracy to the desired joint variables; $x_d = [x_d, \dot{x}_d, \ddot{x}_d, \ldots, x_d^{(n-1)}]^T$, according to actual and desired joint variables, the trucking error vector is defined by [3]:

$$\tilde{x} = x_d - x_a = [\tilde{x}, \ldots, \tilde{x}^{(n-1)}]^T \tag{82}$$

According to the sliding mode controller theory, the main important part to design this controller is sliding surface, a time-varying sliding surface $s(x,t)$ in the state space R^n is given by the following formulation [3]:

$$s(x,t) = (\frac{d}{dt} + \lambda)^{n-1} \tilde{x} = 0 \tag{83}$$

λ is the sliding surface slope coefficient and it is positive constant. The sliding surface can be defined as Proportional-Derivative (PD), Proportional-Integral (PI) and the Proportional-Integral-Derivative (PID). The following formulations represented the three groups are [3]:

$$S_{PD} = \lambda e + \dot{e} \tag{84}$$

$$s(x,t) = (\frac{d}{dt} + \lambda)^{n-1} \left(\int_0^t \tilde{x} \, dt \right) = 0 \tag{85}$$

$$S_{PI} = \lambda e + (\frac{\lambda}{2})^2 \sum e \tag{86}$$

$$S_{PID} = \lambda e + \dot{e} + (\frac{\lambda}{2})^2 \sum e \tag{87}$$

Integral part of sliding surface is used to decrease the steady state error in sliding mode controller. To have the stability and minimum error in sliding mode controller, the main objective is kept the sliding surface slope $s(x,t)$ near to the zero. Therefore, one of the common strategies is to find input U outside of $s(x,t)$ [3].

$$\frac{1}{2}\frac{d}{dt}s^2(x,t) \le -\zeta|s(x,t)| \tag{88}$$

ζ is positive constant.

If $S(0) > 0 \to \dot{S}(t) \le -\zeta$ \hfill (89)

Derivative term of (s) is eliminated by limited integral from t=0 to t=t_{reach}

$$\int_{t=0}^{t=t_{reach}} \dot{S}(t) \le -\int_{t=0}^{t=t_{reach}} \eta \to S(t_{reach}) - S(0) \le -\zeta(t_{reach} - 0) \tag{90}$$

t_{reach} is the time that trajectories reach to the sliding surface. If $S_{t_{reach}} = 0$ the formulation of t_{reach} calculated by;

$$0 - S(0) \le -\eta(t_{reach}) \to t_{reach} \le \frac{S(0)}{\zeta} \tag{91}$$

If $S(0) < 0$

$$0 - S(0) \leq -\eta(t_{reach}) \rightarrow S(0) \leq -\zeta(t_{reach}) \rightarrow t_{reach} \leq \frac{|S(0)|}{\eta} \tag{92}$$

the formulation of (93) guarantees time to reach the sliding surface is smaller than $\frac{|S(0)|}{\zeta}$ since the trajectories are outside of $S(t)$.

$$if \ S_{t_{reach}} = S(0) \rightarrow error(x - x_d) = 0 \tag{93}$$

According to above discussion the formulation of sliding surface (S) is defined as

$$s(x, t) = (\frac{d}{dt} + \lambda) \quad \tilde{x} = (\dot{x} - \dot{x}_d) + \lambda(x - x_d) \tag{94}$$

The change of sliding surface $(\dot{S})$ is;

$$\dot{S} = (\ddot{x} - \ddot{x}_d) + \lambda(\dot{x} - \dot{x}_d) \tag{95}$$

According to the formulation of the second order system, a simple solution to get the sliding condition when the dynamic parameters have uncertainty in parameters or external disturbance is the switching control law:

$$U_{dis} = K(\vec{x}, t) \cdot \text{sgn}(s) \tag{96}$$

The switching function $\text{sgn}(s)$ is defined as

$$sgn(s) = \begin{cases} 1 & s > 0 \\ -1 & s < 0 \\ 0 & s = 0 \end{cases} \tag{97}$$

The $K(\vec{x}, t)$ is the positive constant and the sliding surface can be PD, PI and PID. According to above formulation, the formulation of sliding mode controller for robot manipulator is [3, 7];

$$\tau = \tau_{eq} + \tau_{dis} \tag{98}$$

τ_{eq} is equivalent term of sliding mode controller and this term is related to the nonlinear dynamic formulation of robot manipulator. Conventional sliding mode controller is reliable controller based on the nonlinear dynamic formulation (equivalent part). The switching discontinuous part is introduced by τ_{dis} and this item is the important factor to resistance and robust in this controller. In serial links six degrees of freedom robot manipulator the equivalent part is written as follows;

$$\tau_{eq} = \left[A^{-1}(q) \times (N(q, \dot{q})) + \dot{S} \right] \times A(q) \tag{99}$$

The nonlinear term of $N(q, \dot{q})$ is;

$$[N(q, \dot{q})] = [V(q, \dot{q})] + [G(q)] \tag{100}$$

In PD sliding surface, the change of sliding surface calculated as;

$$S_{PD} = \lambda e + \dot{e} \rightarrow \dot{S}_{PD} = \lambda \dot{e} + \ddot{e} \tag{102}$$

The discontinuous switching term (τ_{dis}) is computed as

$$\tau_{dis} = K \cdot \text{sgn}(S) \tag{103}$$

$$\tau_{dis-PD} = K \cdot \text{sgn}(\lambda e + \dot{e}) \tag{104}$$

$$\tau_{dis-PI} = K \cdot \text{sgn}\left(\lambda e + (\frac{\lambda}{2})^2 \sum e\right) \tag{105}$$

The discontinuous switching part is;

$$\tau_{dis-PID} = K \cdot \text{sgn}\left(\lambda e + \dot{e} + (\frac{\lambda}{2})^2 \sum e\right) \tag{106}$$

$$\tau = \tau_{eq} + K. \text{sgn}(S) = \left[A^{-1}(q) \times (N(q, \dot{q})) + \dot{S} \right] \times A(q) + K. \text{sgn}(S) \tag{107}$$

The formulation of PD-SMC is;

$$\tau_{PD-SMC} = K \cdot \text{sgn}(\lambda e + \dot{e}) + \left[A^{-1}(q) \times (N(q, \dot{q})) + \dot{S}\right] \times A(q) \tag{108}$$

The formulation of PD switching mode discontinuous part of sliding mode controller for 6 DOF serial links robot manipulator is;

$$\begin{bmatrix} \widehat{\tau_{dis-PD}}_1 \\ \widehat{\tau_{dis-PD}}_2 \\ \widehat{\tau_{dis-PD}}_3 \\ \widehat{\tau_{dis-PD}}_4 \\ \widehat{\tau_{dis-PD}}_5 \\ \widehat{\tau_{dis-PD}}_6 \end{bmatrix} = \begin{bmatrix} K_1 \\ K_2 \\ K_3 \\ K_4 \\ K_5 \\ K_6 \end{bmatrix} \times [sgn] \begin{bmatrix} \lambda_1 e_1 + \dot{e}_1 \\ \lambda_2 e_2 + \dot{e}_2 \\ \lambda_3 e_3 + \dot{e}_3 \\ \lambda_4 e_4 + \dot{e}_4 \\ \lambda_5 e_5 + \dot{e}_5 \\ \lambda_6 e_6 + \dot{e}_6 \end{bmatrix} \tag{109}$$

The formulation of equivalent nonlinear part of sliding mode controller for 6 DOF serial links robot manipulator is;

$$\begin{bmatrix} \tau_{eq1} \\ \tau_{eq2} \\ \tau_{eq3} \\ \tau_{eq4} \\ \tau_{eq5} \\ \tau_{eq6} \end{bmatrix} =$$

$$\left[\begin{bmatrix} A_{11} & A_{12} & A_{13} & 0 & 0 & 0 \\ A_{21} & A_{22} & A_{23} & 0 & 0 & 0 \\ A_{31} & A_{32} & A_{33} & 0 & A_{35} & 0 \\ 0 & 0 & 0 & A_{44} & 0 & 0 \\ 0 & 0 & 0 & 0 & A_{55} & 0 \\ 0 & 0 & 0 & 0 & 0 & A_{66} \end{bmatrix}^{-1} \times \left(\begin{bmatrix} b_{112}\dot{q}_1\dot{q}_2 + b_{113}\dot{q}_1\dot{q}_3 + 0 + b_{123}\dot{q}_2\dot{q}_3 \\ 0 + b_{223}\dot{q}_2\dot{q}_3 + 0 + 0 \\ 0 \\ b_{412}\dot{q}_1\dot{q}_2 + b_{413}\dot{q}_1\dot{q}_3 + 0 + 0 \\ 0 \\ 0 \end{bmatrix} + \right.\right.$$

$$\left.\left. \begin{bmatrix} C_{12}\dot{q}_2^2 + C_{13}\dot{q}_3^2 \\ C_{21}\dot{q}_1^2 + C_{23}\dot{q}_3^2 \\ C_{31}\dot{q}_1^2 + C_{32}\dot{q}_2^2 \\ 0 \\ C_{51}\dot{q}_1^2 + C_{52}\dot{q}_2^2 \\ 0 \end{bmatrix} + \begin{bmatrix} 0 \\ g_2 \\ g_3 \\ 0 \\ g_5 \\ 0 \end{bmatrix}\right) + \begin{bmatrix} \dot{S}_1 \\ \dot{S}_2 \\ \dot{S}_3 \\ \dot{S}_4 \\ \dot{S}_5 \\ \dot{S}_6 \end{bmatrix}\right] \times \begin{bmatrix} A_{11} & A_{12} & A_{13} & 0 & 0 & 0 \\ A_{21} & A_{22} & A_{23} & 0 & 0 & 0 \\ A_{31} & A_{32} & A_{33} & 0 & A_{35} & 0 \\ 0 & 0 & 0 & A_{44} & 0 & 0 \\ 0 & 0 & 0 & 0 & A_{55} & 0 \\ 0 & 0 & 0 & 0 & 0 & A_{66} \end{bmatrix} \tag{110}$$

The formulation of Proportional-Derivative (PD) sliding mode controller (SMC) for 6 DOF serial links robot manipulator computed as follows;

$$\begin{bmatrix} \widehat{\tau}_1 \\ \widehat{\tau}_2 \\ \widehat{\tau}_3 \\ \widehat{\tau}_4 \\ \widehat{\tau}_5 \\ \widehat{\tau}_6 \end{bmatrix} = \begin{bmatrix} \widehat{\tau_{dis-PD}}_1 \\ \widehat{\tau_{dis-PD}}_2 \\ \widehat{\tau_{dis-PD}}_3 \\ \widehat{\tau_{dis-PD}}_4 \\ \widehat{\tau_{dis-PD}}_5 \\ \widehat{\tau_{dis-PD}}_6 \end{bmatrix} + \begin{bmatrix} \tau_{eq1} \\ \tau_{eq2} \\ \tau_{eq3} \\ \tau_{eq4} \\ \tau_{eq5} \\ \tau_{eq6} \end{bmatrix} \tag{111}$$

The formulation of PD SMC for 6-DOF serial links robot manipulator is;

$$\begin{bmatrix} \widehat{\tau}_1 \\ \widehat{\tau}_2 \\ \widehat{\tau}_3 \\ \widehat{\tau}_4 \\ \widehat{\tau}_5 \\ \widehat{\tau}_6 \end{bmatrix} = \begin{bmatrix} K_1 \\ K_2 \\ K_3 \\ K_4 \\ K_5 \\ K_6 \end{bmatrix} \times [sgn] \begin{bmatrix} \lambda_1 e_1 + \dot{e}_1 \\ \lambda_2 e_2 + \dot{e}_2 \\ \lambda_3 e_3 + \dot{e}_3 \\ \lambda_4 e_4 + \dot{e}_4 \\ \lambda_5 e_5 + \dot{e}_5 \\ \lambda_6 e_6 + \dot{e}_6 \end{bmatrix} \tag{112}$$

$$+ \left[\begin{matrix} A_{11} & A_{12} & A_{13} & 0 & 0 & 0 \\ A_{21} & A_{22} & A_{23} & 0 & 0 & 0 \\ A_{31} & A_{32} & A_{33} & 0 & A_{35} & 0 \\ 0 & 0 & 0 & A_{44} & 0 & 0 \\ 0 & 0 & 0 & 0 & A_{55} & 0 \\ 0 & 0 & 0 & 0 & 0 & A_{66} \end{matrix} \right]^{-1}$$

$$\times \left(\left[\begin{matrix} b_{112}\dot{q}_1\dot{q}_2 + b_{113}\dot{q}_1\dot{q}_3 + 0 + b_{123}\dot{q}_2\dot{q}_3 \\ 0 + b_{223}\dot{q}_2\dot{q}_3 + 0 + 0 \\ 0 \\ b_{412}\dot{q}_1\dot{q}_2 + b_{413}\dot{q}_1\dot{q}_3 + 0 + 0 \\ 0 \\ 0 \end{matrix} \right] + \left[\begin{matrix} C_{12}\dot{q}_2{}^2 + C_{13}\dot{q}_3{}^2 \\ C_{21}\dot{q}_1{}^2 + C_{23}\dot{q}_3{}^2 \\ C_{31}\dot{q}_1{}^2 + C_{32}\dot{q}_2{}^2 \\ 0 \\ C_{51}\dot{q}_1{}^2 + C_{52}\dot{q}_2{}^2 \\ 0 \end{matrix} \right] + \left[\begin{matrix} 0 \\ g_2 \\ g_3 \\ 0 \\ g_5 \\ 0 \end{matrix} \right] \right)$$

$$+ \left[\begin{matrix} \dot{S}_1 \\ \dot{S}_2 \\ \dot{S}_3 \\ \dot{S}_4 \\ \dot{S}_5 \\ \dot{S}_6 \end{matrix} \right] \times \left[\begin{matrix} A_{11} & A_{12} & A_{13} & 0 & 0 & 0 \\ A_{21} & A_{22} & A_{23} & 0 & 0 & 0 \\ A_{31} & A_{32} & A_{33} & 0 & A_{35} & 0 \\ 0 & 0 & 0 & A_{44} & 0 & 0 \\ 0 & 0 & 0 & 0 & A_{55} & 0 \\ 0 & 0 & 0 & 0 & 0 & A_{66} \end{matrix} \right]$$

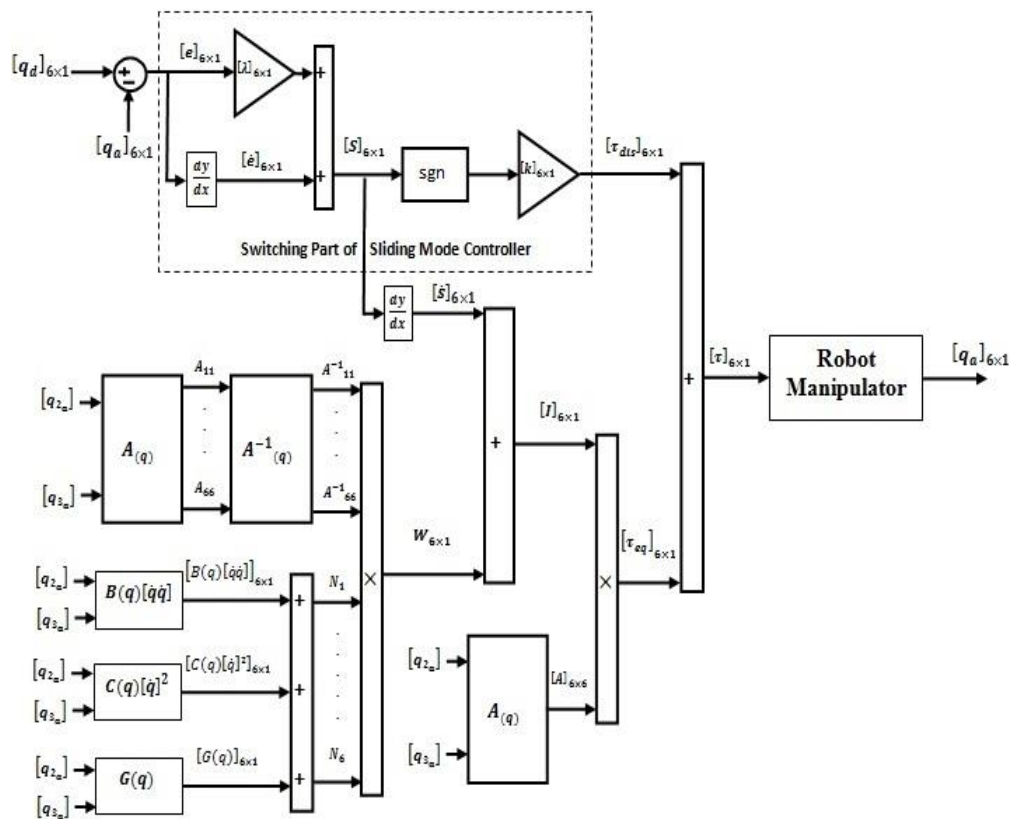Figure 8 shows the PD sliding mode controller for serial links robot manipulator.

Figure 8. Block Diagram of PD Sliding Mode Controller for Robot Manipulator

The PI sliding mode controller is arranged by;

$$\tau_{PI-SMC} = K \cdot \mathbf{sgn}\left(\lambda e + \left(\tfrac{\lambda}{2}\right)^2 \textstyle\sum e\right) + \left[A^{-1}(q) \times (N(q,\dot{q})) + \dot{S}\right] \times A(q) \tag{113}$$

The formulation of PI switching mode discontinuous part of sliding mode controller for 6 DOF serial links robot manipulator is;

$$
\begin{bmatrix} \widehat{\tau_{dis-PI_1}} \\ \widehat{\tau_{dis-PI_2}} \\ \widehat{\tau_{dis-PI_3}} \\ \widehat{\tau_{dis-PI_4}} \\ \widehat{\tau_{dis-PI_5}} \\ \widehat{\tau_{dis-PI_6}} \end{bmatrix} = \begin{bmatrix} K_1 \\ K_2 \\ K_3 \\ K_4 \\ K_5 \\ K_6 \end{bmatrix} \times [sgn] \begin{bmatrix} \lambda_1 e_1 + (\frac{\lambda_1}{2})^2 \sum e_1 \\ \lambda_2 e_2 + (\frac{\lambda_2}{2})^2 \sum e_2 \\ \lambda_3 e_3 + (\frac{\lambda_3}{2})^2 \sum e_3 \\ \lambda_4 e_4 + (\frac{\lambda_4}{2})^2 \sum e_4 \\ \lambda_5 e_5 + (\frac{\lambda_5}{2})^2 \sum e_5 \\ \lambda_6 e_6 + (\frac{\lambda_6}{2})^2 \sum e_6 \end{bmatrix} \tag{114}
$$

The formulation of equivalent nonlinear part of sliding mode controller for 6 DOF serial links robot manipulator is;

$$
\begin{bmatrix} \tau_{eq1} \\ \tau_{eq2} \\ \tau_{eq3} \\ \tau_{eq4} \\ \tau_{eq5} \\ \tau_{eq6} \end{bmatrix} =
$$

$$
\begin{bmatrix} A_{11} & A_{12} & A_{13} & 0 & 0 & 0 \\ A_{21} & A_{22} & A_{23} & 0 & 0 & 0 \\ A_{31} & A_{32} & A_{33} & 0 & A_{35} & 0 \\ 0 & 0 & 0 & A_{44} & 0 & 0 \\ 0 & 0 & 0 & 0 & A_{55} & 0 \\ 0 & 0 & 0 & 0 & 0 & A_{66} \end{bmatrix}^{-1} \left(\begin{bmatrix} b_{112}\dot{q}_1\dot{q}_2 + b_{113}\dot{q}_1\dot{q}_3 + 0 + b_{123}\dot{q}_2\dot{q}_3 \\ 0 + b_{223}\dot{q}_2\dot{q}_3 + 0 + 0 \\ 0 \\ b_{412}\dot{q}_1\dot{q}_2 + b_{413}\dot{q}_1\dot{q}_3 + 0 + 0 \\ 0 \\ 0 \end{bmatrix} + \right.
$$

$$
\left. \begin{bmatrix} C_{12}\dot{q}_2{}^2 + C_{13}\dot{q}_3{}^2 \\ C_{21}\dot{q}_1{}^2 + C_{23}\dot{q}_3{}^2 \\ C_{31}\dot{q}_1{}^2 + C_{32}\dot{q}_2{}^2 \\ 0 \\ C_{51}\dot{q}_1{}^2 + C_{52}\dot{q}_2{}^2 \\ 0 \end{bmatrix} + \begin{bmatrix} 0 \\ g_2 \\ g_3 \\ 0 \\ g_5 \\ 0 \end{bmatrix} \right) + \begin{bmatrix} \dot{S}_1 \\ \dot{S}_2 \\ \dot{S}_3 \\ \dot{S}_4 \\ \dot{S}_5 \\ \dot{S}_6 \end{bmatrix}] \times \begin{bmatrix} A_{11} & A_{12} & A_{13} & 0 & 0 & 0 \\ A_{21} & A_{22} & A_{23} & 0 & 0 & 0 \\ A_{31} & A_{32} & A_{33} & 0 & A_{35} & 0 \\ 0 & 0 & 0 & A_{44} & 0 & 0 \\ 0 & 0 & 0 & 0 & A_{55} & 0 \\ 0 & 0 & 0 & 0 & 0 & A_{66} \end{bmatrix} \tag{115}
$$

The formulation of Proportional-Integral (PI) sliding mode controller (SMC) for 6 DOF serial links robot manipulator computed as follows;

$$
\begin{bmatrix} \widehat{\tau_1} \\ \widehat{\tau_2} \\ \widehat{\tau_3} \\ \widehat{\tau_4} \\ \widehat{\tau_5} \\ \widehat{\tau_6} \end{bmatrix} = \begin{bmatrix} \widehat{\tau_{dis-PI_1}} \\ \widehat{\tau_{dis-PI_2}} \\ \widehat{\tau_{dis-PI_3}} \\ \widehat{\tau_{dis-PI_4}} \\ \widehat{\tau_{dis-PI_5}} \\ \widehat{\tau_{dis-PI_6}} \end{bmatrix} + \begin{bmatrix} \tau_{eq1} \\ \tau_{eq2} \\ \tau_{eq3} \\ \tau_{eq4} \\ \tau_{eq5} \\ \tau_{eq6} \end{bmatrix} \tag{116}
$$

The formulation of PI SMC for 6-DOF serial links robot manipulator is;

$$
\begin{bmatrix} \widehat{\tau_1} \\ \widehat{\tau_2} \\ \widehat{\tau_3} \\ \widehat{\tau_4} \\ \widehat{\tau_5} \\ \widehat{\tau_6} \end{bmatrix} = \begin{bmatrix} K_1 \\ K_2 \\ K_3 \\ K_4 \\ K_5 \\ K_6 \end{bmatrix} \times [sgn] \begin{bmatrix} \lambda_1 e_1 + (\frac{\lambda_1}{2})^2 \sum e_1 \\ \lambda_2 e_2 + (\frac{\lambda_2}{2})^2 \sum e_2 \\ \lambda_3 e_3 + (\frac{\lambda_3}{2})^2 \sum e_3 \\ \lambda_4 e_4 + (\frac{\lambda_4}{2})^2 \sum e_4 \\ \lambda_5 e_5 + (\frac{\lambda_5}{2})^2 \sum e_5 \\ \lambda_6 e_6 + (\frac{\lambda_6}{2})^2 \sum e_6 \end{bmatrix} \tag{117}
$$

$$+ \left[\begin{matrix} A_{11} & A_{12} & A_{13} & 0 & 0 & 0 \\ A_{21} & A_{22} & A_{23} & 0 & 0 & 0 \\ A_{31} & A_{32} & A_{33} & 0 & A_{35} & 0 \\ 0 & 0 & 0 & A_{44} & 0 & 0 \\ 0 & 0 & 0 & 0 & A_{55} & 0 \\ 0 & 0 & 0 & 0 & 0 & A_{66} \end{matrix}\right]^{-1} \times$$

$$\left(\left[\begin{matrix} b_{112}\dot{q}_1\dot{q}_2 + b_{113}\dot{q}_1\dot{q}_3 + 0 + b_{123}\dot{q}_2\dot{q}_3 \\ 0 + b_{223}\dot{q}_2\dot{q}_3 + 0 + 0 \\ 0 \\ b_{412}\dot{q}_1\dot{q}_2 + b_{413}\dot{q}_1\dot{q}_3 + 0 + 0 \\ 0 \\ 0 \end{matrix}\right] + \left[\begin{matrix} C_{12}\dot{q}_2{}^2 + C_{13}\dot{q}_3{}^2 \\ C_{21}\dot{q}_1{}^2 + C_{23}\dot{q}_3{}^2 \\ C_{31}\dot{q}_1{}^2 + C_{32}\dot{q}_2{}^2 \\ 0 \\ C_{51}\dot{q}_1{}^2 + C_{52}\dot{q}_2{}^2 \\ 0 \end{matrix}\right] + \left[\begin{matrix} 0 \\ g_2 \\ g_3 \\ 0 \\ g_5 \\ 0 \end{matrix}\right]\right) + \left[\begin{matrix} \dot{S}_1 \\ \dot{S}_2 \\ \dot{S}_3 \\ \dot{S}_4 \\ \dot{S}_5 \\ \dot{S}_6 \end{matrix}\right] \right] \times$$

$$\left[\begin{matrix} A_{11} & A_{12} & A_{13} & 0 & 0 & 0 \\ A_{21} & A_{22} & A_{23} & 0 & 0 & 0 \\ A_{31} & A_{32} & A_{33} & 0 & A_{35} & 0 \\ 0 & 0 & 0 & A_{44} & 0 & 0 \\ 0 & 0 & 0 & 0 & A_{55} & 0 \\ 0 & 0 & 0 & 0 & 0 & A_{66} \end{matrix}\right]$$

Figure 9 shows the block diagram of PI sliding mode controller for serial links robot manipulator.
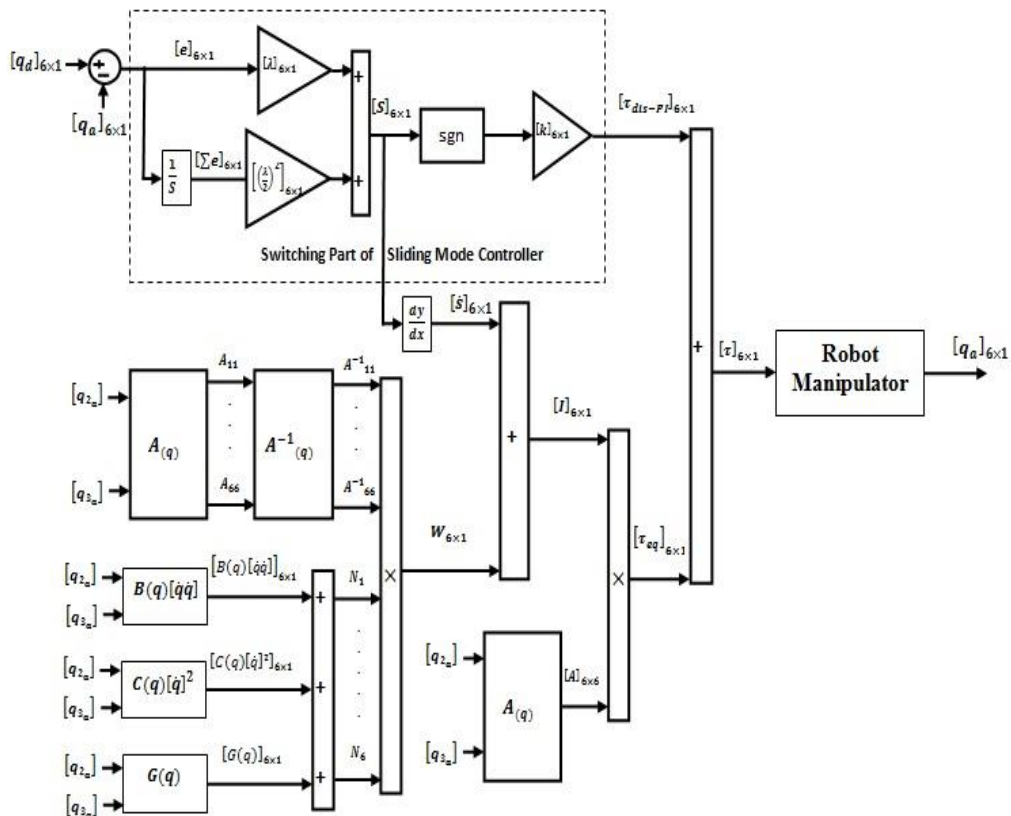

Figure 9. Block Diagram of PI Sliding Mode Controller for Robot Manipulator

The PID sliding mode controller is written

$$\tau_{PID-SMC} = K \cdot \text{sgn}\left(\lambda e + \dot{e} + \left(\frac{\lambda}{2}\right)^2 \sum e\right) + \left[A^{-1}(q) \times \left(N(q,\dot{q})\right) + \dot{S}\right] \times A(q) \tag{118}$$

The formulation of PID switching mode discontinuous part of sliding mode controller for 6 DOF serial links robot manipulator is;

$$
\begin{bmatrix} \widehat{\tau_{dis-PI_1}} \\ \widehat{\tau_{dis-PI_2}} \\ \widehat{\tau_{dis-PI_3}} \\ \widehat{\tau_{dis-PI_4}} \\ \widehat{\tau_{dis-PI_5}} \\ \widehat{\tau_{dis-PI_6}} \end{bmatrix} = \begin{bmatrix} K_1 \\ K_2 \\ K_3 \\ K_4 \\ K_5 \\ K_6 \end{bmatrix} \times [sgn] \begin{bmatrix} \lambda_1 e_1 + \dot{e}_1 + (\frac{\lambda_1}{2})^2 \sum e_1 \\ \lambda_2 e_2 + \dot{e}_2 + (\frac{\lambda_2}{2})^2 \sum e_2 \\ \lambda_3 e_3 + \dot{e}_3 + (\frac{\lambda_3}{2})^2 \sum e_3 \\ \lambda_4 e_4 + \dot{e}_4 + (\frac{\lambda_4}{2})^2 \sum e_4 \\ \lambda_5 e_5 + \dot{e}_5 + (\frac{\lambda_5}{2})^2 \sum e_5 \\ \lambda_6 e_6 + \dot{e}_6 + (\frac{\lambda_6}{2})^2 \sum e_6 \end{bmatrix} \tag{119}
$$

The formulation of equivalent nonlinear part of sliding mode controller for 6 DOF serial links robot manipulator is;

$$
\begin{bmatrix} \tau_{eq1} \\ \tau_{eq2} \\ \tau_{eq3} \\ \tau_{eq4} \\ \tau_{eq5} \\ \tau_{eq6} \end{bmatrix} =
$$

$$
[\begin{bmatrix} A_{11} & A_{12} & A_{13} & 0 & 0 & 0 \\ A_{21} & A_{22} & A_{23} & 0 & 0 & 0 \\ A_{31} & A_{32} & A_{33} & 0 & A_{35} & 0 \\ 0 & 0 & 0 & A_{44} & 0 & 0 \\ 0 & 0 & 0 & 0 & A_{55} & 0 \\ 0 & 0 & 0 & 0 & 0 & A_{66} \end{bmatrix}^{-1} \times (\begin{bmatrix} b_{112}\dot{q}_1\dot{q}_2 + b_{113}\dot{q}_1\dot{q}_3 + 0 + b_{123}\dot{q}_2\dot{q}_3 \\ 0 + b_{223}\dot{q}_2\dot{q}_3 + 0 + 0 \\ 0 \\ b_{412}\dot{q}_1\dot{q}_2 + b_{413}\dot{q}_1\dot{q}_3 + 0 + 0 \\ 0 \\ 0 \end{bmatrix} +
$$

$$
\begin{bmatrix} C_{12}\dot{q}_2^2 + C_{13}\dot{q}_3^2 \\ C_{21}\dot{q}_1^2 + C_{23}\dot{q}_3^2 \\ C_{31}\dot{q}_1^2 + C_{32}\dot{q}_2^2 \\ 0 \\ C_{51}\dot{q}_1^2 + C_{52}\dot{q}_2^2 \\ 0 \end{bmatrix} + \begin{bmatrix} 0 \\ g_2 \\ g_3 \\ 0 \\ g_5 \\ 0 \end{bmatrix}) + \begin{bmatrix} \dot{S}_1 \\ \dot{S}_2 \\ \dot{S}_3 \\ \dot{S}_4 \\ \dot{S}_5 \\ \dot{S}_6 \end{bmatrix}] \times \begin{bmatrix} A_{11} & A_{12} & A_{13} & 0 & 0 & 0 \\ A_{21} & A_{22} & A_{23} & 0 & 0 & 0 \\ A_{31} & A_{32} & A_{33} & 0 & A_{35} & 0 \\ 0 & 0 & 0 & A_{44} & 0 & 0 \\ 0 & 0 & 0 & 0 & A_{55} & 0 \\ 0 & 0 & 0 & 0 & 0 & A_{66} \end{bmatrix} \tag{120}
$$

The formulation of Proportional-Integral (PID) sliding mode controller (SMC) for 6 DOF serial links robot manipulator computed as follows;

$$
\begin{bmatrix} \widehat{\tau_1} \\ \widehat{\tau_2} \\ \widehat{\tau_3} \\ \widehat{\tau_4} \\ \widehat{\tau_5} \\ \widehat{\tau_6} \end{bmatrix} = \begin{bmatrix} \widehat{\tau_{dis-PID_1}} \\ \widehat{\tau_{dis-PID_2}} \\ \widehat{\tau_{dis-PID_3}} \\ \widehat{\tau_{dis-PID_4}} \\ \widehat{\tau_{dis-PID_5}} \\ \widehat{\tau_{dis-PID_6}} \end{bmatrix} + \begin{bmatrix} \tau_{eq1} \\ \tau_{eq2} \\ \tau_{eq3} \\ \tau_{eq4} \\ \tau_{eq5} \\ \tau_{eq6} \end{bmatrix} \tag{121}
$$

The formulation of PID SMC for 6-DOF serial links robot manipulator is;

$$
\begin{bmatrix} \widehat{\tau_1} \\ \widehat{\tau_2} \\ \widehat{\tau_3} \\ \widehat{\tau_4} \\ \widehat{\tau_5} \\ \widehat{\tau_6} \end{bmatrix} = \begin{bmatrix} K_1 \\ K_2 \\ K_3 \\ K_4 \\ K_5 \\ K_6 \end{bmatrix} \times [sgn] \begin{bmatrix} \lambda_1 e_1 + \dot{e}_1 + (\frac{\lambda_1}{2})^2 \sum e_1 \\ \lambda_2 e_2 + \dot{e}_2 + (\frac{\lambda_2}{2})^2 \sum e_2 \\ \lambda_3 e_3 + \dot{e}_3 + (\frac{\lambda_3}{2})^2 \sum e_3 \\ \lambda_4 e_4 + \dot{e}_4 + (\frac{\lambda_4}{2})^2 \sum e_4 \\ \lambda_5 e_5 + \dot{e}_5 + (\frac{\lambda_5}{2})^2 \sum e_5 \\ \lambda_6 e_6 + \dot{e}_6 + (\frac{\lambda_6}{2})^2 \sum e_6 \end{bmatrix} \tag{122}
$$

$$+ \left[\begin{array}{cccccc} A_{11} & A_{12} & A_{13} & 0 & 0 & 0 \\ A_{21} & A_{22} & A_{23} & 0 & 0 & 0 \\ A_{31} & A_{32} & A_{33} & 0 & A_{35} & 0 \\ 0 & 0 & 0 & A_{44} & 0 & 0 \\ 0 & 0 & 0 & 0 & A_{55} & 0 \\ 0 & 0 & 0 & 0 & 0 & A_{66} \end{array} \right]^{-1} \times$$

$$\left(\left[\begin{array}{c} b_{112}\dot{q}_1\dot{q}_2 + b_{113}\dot{q}_1\dot{q}_3 + 0 + b_{123}\dot{q}_2\dot{q}_3 \\ 0 + b_{223}\dot{q}_2\dot{q}_3 + 0 + 0 \\ 0 \\ b_{412}\dot{q}_1\dot{q}_2 + b_{413}\dot{q}_1\dot{q}_3 + 0 + 0 \\ 0 \\ 0 \end{array} \right] + \left[\begin{array}{c} C_{12}\dot{q}_2^2 + C_{13}\dot{q}_3^2 \\ C_{21}\dot{q}_1^2 + C_{23}\dot{q}_3^2 \\ C_{31}\dot{q}_1^2 + C_{32}\dot{q}_2^2 \\ 0 \\ C_{51}\dot{q}_1^2 + C_{52}\dot{q}_2^2 \\ 0 \end{array} \right] + \left[\begin{array}{c} 0 \\ g_2 \\ g_3 \\ 0 \\ g_5 \\ 0 \end{array} \right] \right) + \left[\begin{array}{c} \dot{S}_1 \\ \dot{S}_2 \\ \dot{S}_3 \\ \dot{S}_4 \\ \dot{S}_5 \\ \dot{S}_6 \end{array} \right]] \times$$

$$\left[\begin{array}{cccccc} A_{11} & A_{12} & A_{13} & 0 & 0 & 0 \\ A_{21} & A_{22} & A_{23} & 0 & 0 & 0 \\ A_{31} & A_{32} & A_{33} & 0 & A_{35} & 0 \\ 0 & 0 & 0 & A_{44} & 0 & 0 \\ 0 & 0 & 0 & 0 & A_{55} & 0 \\ 0 & 0 & 0 & 0 & 0 & A_{66} \end{array} \right]$$

Figure 10 demonstrates the block diagram of PID sliding mode controller for serial links robot manipulator.
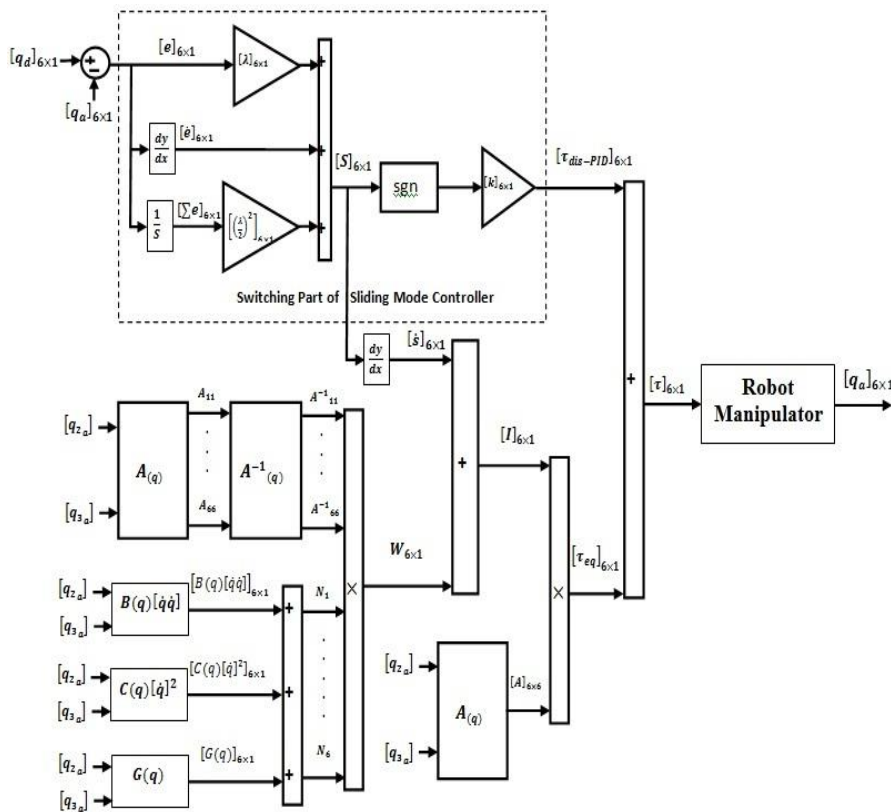

Figure 10. Block Diagram of PID Sliding Mode Controller for Robot Manipulator

Chattering Attenuation Using Proposed Method:

In sliding mode controller select the desired sliding surface and *sign* function play a vital role to system performance and if the dynamic of robot manipulator is derived to

sliding surface then the linearization and decoupling through the use of feedback, not gears, can be realized. In this state, the derivative of sliding surface can help to decoupled and linearized closed-loop PUMA robot dynamics that one expects in computed torque control. Linearization and decoupling by sliding mode controller can be obtained in spite of the quality of the robot manipulator dynamic model, in contrast to the computed-torque control that requires the exact dynamic model of a system. As a result, uncertainties are estimated by discontinuous feedback control but it can cause to chattering. To reduce the chattering in presence of switching functions; linear controller is added to discontinuous part of sliding mode controller. Linear controller is type of stable controller as well as conventional sliding mode controller. In proposed methodology PD, PI or PID linear controller is used in parallel with discontinuous part to reduce the role of sliding surface slope as a main coefficient. The formulation of new chattering free sliding mode controller for robot manipulator is;

$$\tau = \tau_{eq} + \tau_{dis-new} \tag{123}$$

τ_{eq} is equivalent term of sliding mode controller and this term is related to the nonlinear dynamic formulation of robot manipulator. The new switching discontinuous part is introduced by $\tau_{dis-new}$ and this item is the important factor to resistance and robust in this controller. In PD sliding surface, the change of sliding surface calculated as;

$$S_{PD} = \lambda e + \dot{e} \rightarrow \dot{S}_{PD} = \lambda \dot{e} + \ddot{e} \tag{124}$$

The discontinuous switching term (τ_{dis}) is computed as

$$\tau_{dis-new} = K_a \cdot \text{sgn}(S) + K_b . S \tag{125}$$

$$\tau_{dis-PD-new} = K_a \cdot \text{sgn}(\lambda e + \dot{e}) + K_b \cdot (\lambda e + \dot{e}) \tag{126}$$

$$\tau_{dis-PI-new} = K_a \cdot \text{sgn}\left(\lambda e + (\tfrac{\lambda}{2})^2 \sum e\right) + K_b \cdot \left(\lambda e + (\tfrac{\lambda}{2})^2 \sum e\right) \tag{127}$$

$$\tau_{dis-PID-new} = K_a \cdot \text{sgn}\left(\lambda e + \dot{e} + (\tfrac{\lambda}{2})^2 \sum e\right) + K_b \cdot \left(\lambda e + \dot{e} + (\tfrac{\lambda}{2})^2 \sum e\right) \tag{128}$$

$$\tau = \tau_{eq} + K_a . \text{sgn}(S) + + K_b . S = \left[A^{-1}(q) \times (N(q,\dot{q})) + \dot{S}\right] \times A(q) + K_a . \text{sgn}(S) + K_b . S \tag{129}$$

The formulation of PD-SMC is;

$$\tau_{PD-SMC-new} = K_a \cdot \text{sgn}(\lambda e + \dot{e}) + K_b \cdot (\lambda e + \dot{e}) + \left[A^{-1}(q) \times (N(q,\dot{q})) + \dot{S}\right] \times A(q) \tag{130}$$

The formulation of new chattering free PD switching mode discontinuous part of sliding mode controller for 6 DOF serial links robot manipulator is;

$$\begin{bmatrix} \tau_{\widehat{newdis-PD}_1} \\ \tau_{\widehat{newdis-PD}_2} \\ \tau_{\widehat{newdis-PD}_3} \\ \tau_{\widehat{newdis-PD}_4} \\ \tau_{\widehat{newdis-PD}_5} \\ \tau_{\widehat{newdis-PD}_6} \end{bmatrix} = \begin{bmatrix} K_{a1} \\ K_{a2} \\ K_{a3} \\ K_{a4} \\ K_{a5} \\ K_{a6} \end{bmatrix} \times [sgn] \begin{bmatrix} \lambda_1 e_1 + \dot{e}_1 \\ \lambda_2 e_2 + \dot{e}_2 \\ \lambda_3 e_3 + \dot{e}_3 \\ \lambda_4 e_4 + \dot{e}_4 \\ \lambda_5 e_5 + \dot{e}_5 \\ \lambda_6 e_6 + \dot{e}_6 \end{bmatrix} + \begin{bmatrix} K_{b1} \\ K_{b2} \\ K_{b3} \\ K_{b4} \\ K_{b5} \\ K_{b6} \end{bmatrix} \times \begin{bmatrix} \lambda_1 e_1 + \dot{e}_1 \\ \lambda_2 e_2 + \dot{e}_2 \\ \lambda_3 e_3 + \dot{e}_3 \\ \lambda_4 e_4 + \dot{e}_4 \\ \lambda_5 e_5 + \dot{e}_5 \\ \lambda_6 e_6 + \dot{e}_6 \end{bmatrix} \tag{131}$$

The formulation of equivalent nonlinear part of sliding mode controller for 6 DOF serial links robot manipulator is;

$$
\begin{bmatrix} \tau_{eq1} \\ \tau_{eq2} \\ \tau_{eq3} \\ \tau_{eq4} \\ \tau_{eq5} \\ \tau_{eq6} \end{bmatrix} = [\begin{bmatrix} A_{11} & A_{12} & A_{13} & 0 & 0 & 0 \\ A_{21} & A_{22} & A_{23} & 0 & 0 & 0 \\ A_{31} & A_{32} & A_{33} & 0 & A_{35} & 0 \\ 0 & 0 & 0 & A_{44} & 0 & 0 \\ 0 & 0 & 0 & 0 & A_{55} & 0 \\ 0 & 0 & 0 & 0 & 0 & A_{66} \end{bmatrix}^{-1} \times (\begin{bmatrix} b_{112}\dot{q}_1\dot{q}_2 + b_{113}\dot{q}_1\dot{q}_3 + 0 + b_{123}\dot{q}_2\dot{q}_3 \\ 0 + b_{223}\dot{q}_2\dot{q}_3 + 0 + 0 \\ 0 \\ b_{412}\dot{q}_1\dot{q}_2 + b_{413}\dot{q}_1\dot{q}_3 + 0 + 0 \\ 0 \\ 0 \end{bmatrix} +
$$

$$
\begin{bmatrix} C_{12}\dot{q}_2{}^2 + C_{13}\dot{q}_3{}^2 \\ C_{21}\dot{q}_1{}^2 + C_{23}\dot{q}_3{}^2 \\ C_{31}\dot{q}_1{}^2 + C_{32}\dot{q}_2{}^2 \\ 0 \\ C_{51}\dot{q}_1{}^2 + C_{52}\dot{q}_2{}^2 \\ 0 \end{bmatrix} + \begin{bmatrix} 0 \\ g_2 \\ g_3 \\ 0 \\ g_5 \\ 0 \end{bmatrix}) + \begin{bmatrix} \dot{S}_1 \\ \dot{S}_2 \\ \dot{S}_3 \\ \dot{S}_4 \\ \dot{S}_5 \\ \dot{S}_6 \end{bmatrix}] \times \begin{bmatrix} A_{11} & A_{12} & A_{13} & 0 & 0 & 0 \\ A_{21} & A_{22} & A_{23} & 0 & 0 & 0 \\ A_{31} & A_{32} & A_{33} & 0 & A_{35} & 0 \\ 0 & 0 & 0 & A_{44} & 0 & 0 \\ 0 & 0 & 0 & 0 & A_{55} & 0 \\ 0 & 0 & 0 & 0 & 0 & A_{66} \end{bmatrix} \qquad (132)
$$

The formulation of new chattering free Proportional-Derivative (PD) sliding mode controller (SMC) for 6 DOF serial links robot manipulator computed as follows;

$$
\begin{bmatrix} \widehat{\tau_1} \\ \widehat{\tau_2} \\ \widehat{\tau_3} \\ \widehat{\tau_4} \\ \widehat{\tau_5} \\ \widehat{\tau_6} \end{bmatrix} = \begin{bmatrix} \widehat{\tau_{newdis-PD_1}} \\ \widehat{\tau_{newdis-PD_2}} \\ \widehat{\tau_{newdis-PD_3}} \\ \widehat{\tau_{newdis-PD_4}} \\ \widehat{\tau_{newdis-PD_5}} \\ \widehat{\tau_{newdis-PD_6}} \end{bmatrix} + \begin{bmatrix} \tau_{eq1} \\ \tau_{eq2} \\ \tau_{eq3} \\ \tau_{eq4} \\ \tau_{eq5} \\ \tau_{eq6} \end{bmatrix} \qquad (133)
$$

Figure 11 shows the new chattering free PD sliding mode controller for serial links robot manipulator.
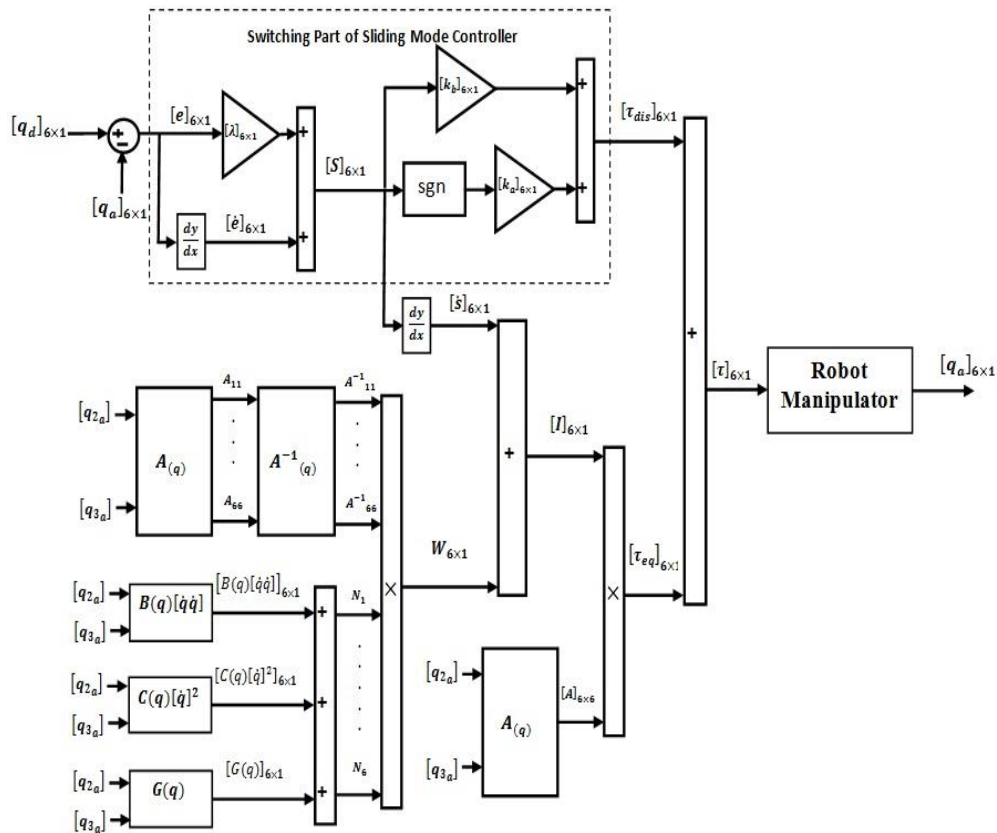

Figure 11. Block Diagram of Chatter-free Proposed Sliding Mode Controller for Robot Manipulator

Design FPGA-Based Improved Sliding Mode Controller:

In this research design a new Microelectronic device to improve the flexibility, speed and reduce the error. To achieve to these goals, Spartan 3E FPGA is selected. The information of this device is introduced as the following Table 5.

Table 5. Summary of XA Spartan-3E FPGA Attributes

Device	System Gates	Equivalent Logic Cells	CLB Array (One CLB = Four Slices)				Distributed RAM bits[1]	Block RAM bits[1]	Dedicated Multipliers	DCMs	Maximum User I/O	Maximum Differential I/O Pairs
			Rows	Columns	Total CLBs	Total Slices						
XA3S100E	100K	2,160	22	16	240	960	15K	72K	4	2	108	40
XA3S250E	250K	5,508	34	26	612	2,448	38K	216K	12	4	172	68
XA3S500E	500K	10,476	46	34	1,164	4,656	73K	360K	20	4	190	77
XA3S1200E	1200K	19,512	60	46	2,168	8,672	136K	504K	28	8	304	124
XA3S1600E	1600K	33,192	76	58	3,688	14,752	231K	648K	36	8	376	156

Notes:
1. By convention, one Kb is equivalent to 1,024 bits.

Regarding to research design, this design has the following steps:
- design Derivative algorithm
- design PD algorithm
- design nonlinear function algorithm
- design Proposed Partly Sliding Mode Controller

The following formulation shows the derivative algorithm:

$$d(e) = \frac{Din(t) - Din(t-1)}{\Delta t} = \big(Din(k+1) - Din(k)\big) \times sample\ time \qquad (134)$$

The following Figures (Figure 12 and Figure 13) show the outline and interior view of derivative design in HDL. Regarding to this Figure this system has 40 bits-inputs and 40 bits-output.
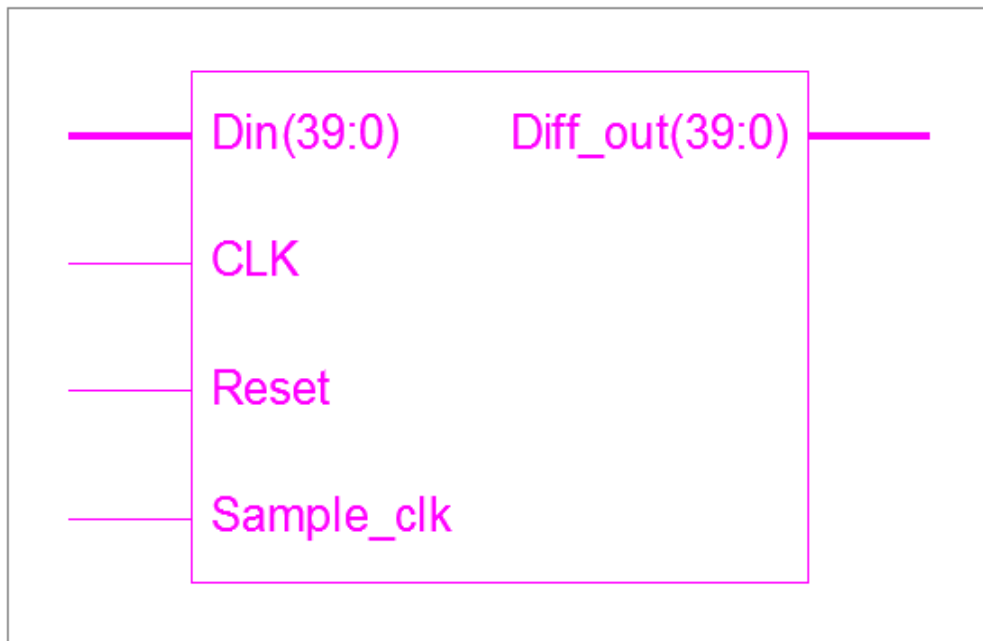

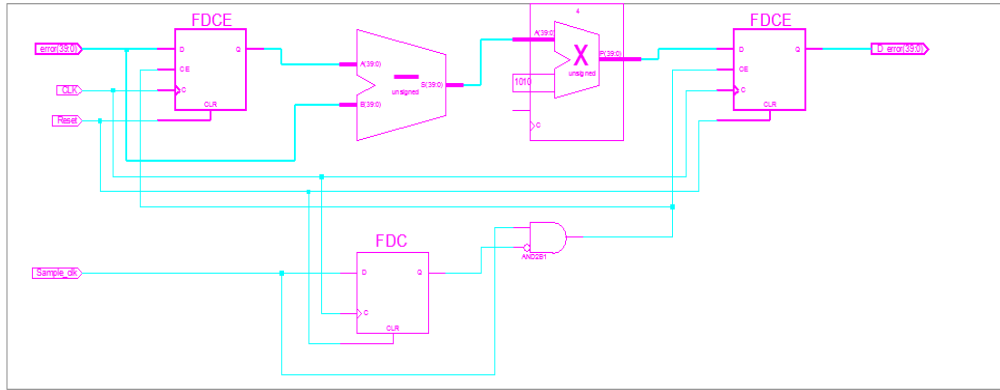**Figure 12. Outline Derivative Algorithm in HDL using Spartan 3E**

Figure 13. Interior View: Derivative Algorithm in HDL using Spartan 3E

The following Figure (Figure 14) shows the Derivative Program based on VHDL code.

```
entity Derivative_control is
    Port(error : in  STD_LOGIC_VECTOR (39 downto 0);
         D_error : out  STD_LOGIC_VECTOR (39 downto 0);
         Reset : in  STD_LOGIC;
         CLK : in  STD_LOGIC;
         Sample_clk : in  STD_LOGIC);
end Derivative_control;

architecture Behavioral of Derivative_control is
-------------------------------------------------------------------------
constant sample_rate : std_logic_vector(4 downto 0) := "01010";
signal last_error : std_logic_vector(39 downto 0);
signal data_sample_error : std_logic_vector(39 downto 0);
signal diff_data : std_logic_vector(44 downto 0);
signal last_sample_clk : std_logic;
signal sample_clk_edge : std_logic;
-------------------------------------------------------------------------
begin
-------------------------------------------------------------------------
sample_clk_edge <= (not last_sample_clk) and Sample_clk;
process(CLK, Reset)
begin
    if(Reset = '1')then
        last_sample_clk <= '0';
    elsif(rising_edge(CLK))then
        last_sample_clk <= Sample_clk;
    end if;
end process;
-------------------------------------------------------------------------
process(CLK)
begin
    if(Reset = '1')then
        last_error <= (others => '0');
        D_error <= (others => '0');
    elsif(rising_edge(CLK) and sample_clk_edge = '1')then
```

Figure 14. VHDL Code: Derivative Algorithm in HDL Spartan 3E Device

The Formulation of PD control is as follows:

$$U_{PID} = K_p \times e + K_v \left(\frac{de}{dt}\right) = K_p \times e + K_v \dot{e} \tag{135}$$

The following Figures (Figure 15 and Figure 16) show the outline and interior view of PD control design in HDL. Regarding to this Figure this system has 30 bits-inputs and 35 bits-output.
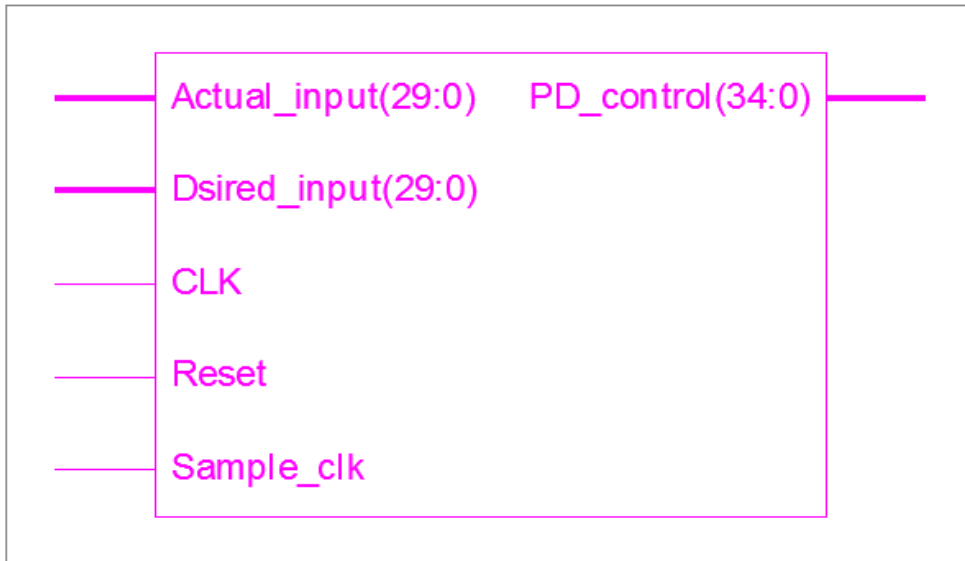
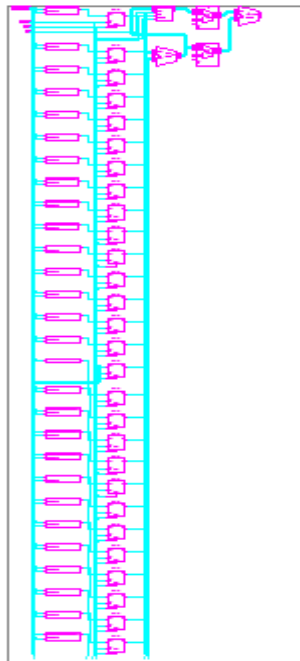**Figure 15. Outline PD Algorithm in HDL Spartan 3E Device**

Figure 16. Interior View: PD Algorithm in HDL Spartan 3E Device

The following Figure (Figure 17) shows the PD Program based on VHDL code.

```
entity PD_Controler is
    Generic(Kp : std_logic_vector(7 downto 0) := B"11111010";
            Kv : std_logic_vector(7 downto 0) := B"00111100");
    Port(Actual_input : in  STD_LOGIC_VECTOR (29 downto 0);
      Dsired_input : in  STD_LOGIC_VECTOR (29 downto 0);
      PD_control : out  STD_LOGIC_VECTOR (34 downto 0);
      Reset : in  STD_LOGIC;
      CLK : in  STD_LOGIC;
      Sample_clk : in  STD_LOGIC);
end PD_Controler;
-------------------------------------------------------------------------------
architecture Behavioral of PD_Controler is
-------------------------------------------------------------------------------
------Signals definitions
-------------------------------------------------------------------------------
signal Actual_input_buf : std_logic_vector(39 downto 0);
signal Desired_input_buf : std_logic_vector(39 downto 0);
signal Error_gain : std_logic_vector(47 downto 0);
signal Error_diff : std_logic_vector(39 downto 0);
signal Error : std_logic_vector(39 downto 0);
signal Error_diff_gain : std_logic_vector(47 downto 0);
signal PD_control_buf : std_logic_vector(39 downto 0);
-------------------------------------------------------------------------------
------------Numerical Differential calculator
COMPONENT Derivative_control
  PORT(
    error : IN std_logic_vector(39 downto 0);
    Reset : IN std_logic;
    CLK : IN std_logic;
    Sample_clk : IN std_logic;
    D_error : OUT std_logic_vector(39 downto 0)
    );
  END COMPONENT;
```

Figure 17. VHDL Code: PD Algorithm in HDL Spartan 3E Device

The Formulation of *sgn* nonlinear function is as follows:

$$sgn(S) = \begin{cases} 1 & \left(s/\emptyset > 1\right) \\ -1 & \left(s/\emptyset < -1\right) \end{cases} \tag{136}$$

The following Figures (Figure 18 and Figure 19) show the outline and interior view of sgn nonlinear function design in HDL. Regarding to this Figure this system has 40 bits-inputs and 40 bits-output.
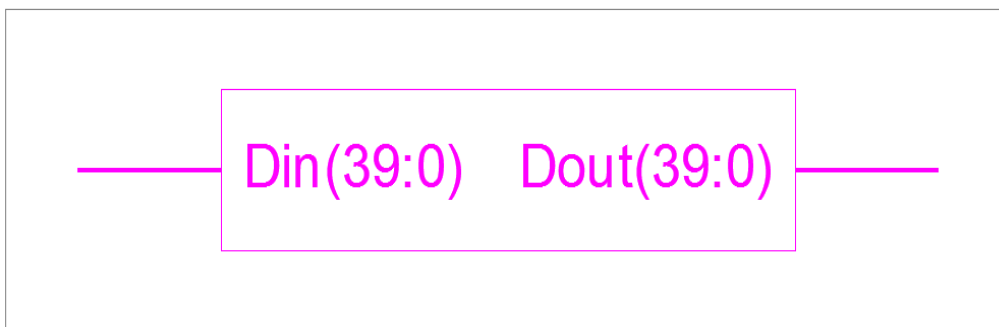

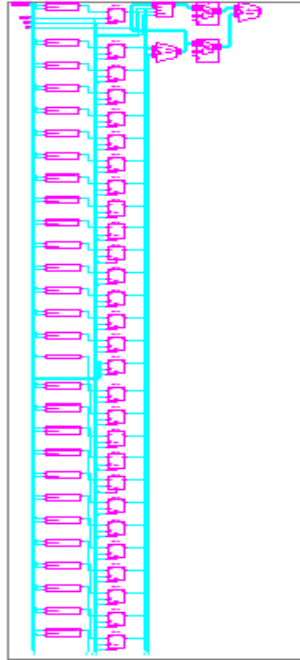**Figure 18. Outline sgn Algorithm in HDL Spartan 3E Device**

Figure 19. Interior View: Nonlinear Function Algorithm in HDL Spartan 3E Device

The Formulation of *proposed controller* is as follows:

$$U = k.sgn(s) + k.s \tag{137}$$

The following Figures (Figure 20 and Figure 21) show the outline and interior view of proposed controller design in HDL. Regarding to this Figure this system has 30 bits-inputs and 35 bits-output.

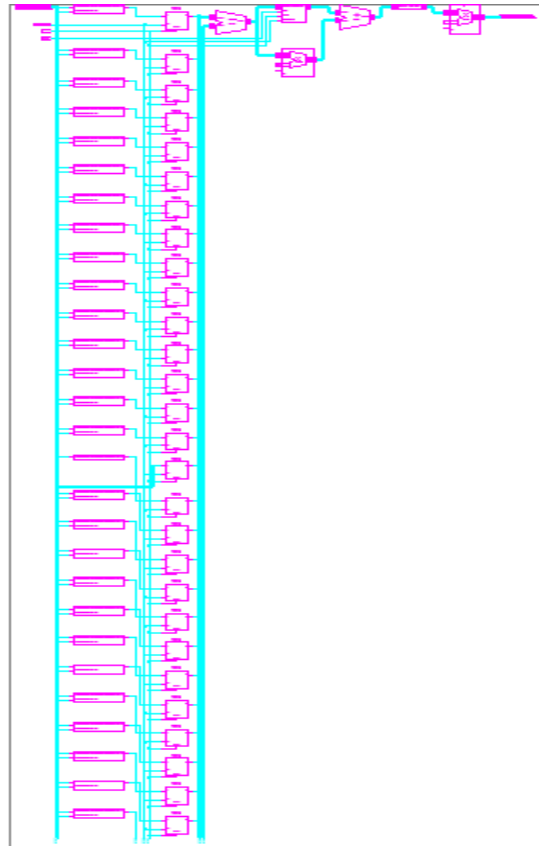**Figure 20. Outline Proposed Algorithm in HDL Spartan 3E Device**

Figure 21. Interior View: Proposed Algorithm in HDL Spartan 3E Device

The summary of proposed method shows in the following Figure (Figure 22).

Device Utilization Summary				
Logic Utilization	**Used**	**Available**	**Utilization**	**Note(s)**
Number of Slice Flip Flops	216	29,504	1%	
Number of 4 input LUTs	610	29,504	2%	
Logic Distribution				
Number of occupied Slices	342	14,752	2%	
Number of Slices containing only related logic	342	342	100%	
Number of Slices containing unrelated logic	0	342	0%	
Total Number of 4 input LUTs	622	29,504	2%	
Number used as logic	610			
Number used as a route-thru	12			
Number of bonded IOBs	288	376	76%	
IOB Flip Flops	181			
Number of GCLKs	2	24	8%	
Number of MULT18X18SIOs	27	36	75%	
Total equivalent gate count for design	10,334			
Additional JTAG gate count for IOBs	13,824			

Figure 22. Summary of Proposed Method Design

4. Result

In this part, MATLAB based improved sliding mode controller and FPGA-based improved sliding mode controller are test. Figure 23 shows the trajectory following in sliding mode controller and improve sliding mode controller. Regarding to the following Figure, SMC has high frequency oscillation (chattering) in certain condition that improved SMC reduce/eliminate this challenge. Proposed method eliminates the

chattering as well overshoot and undershoot but the main disadvantage of proposed method is rise-time especially in the first link.
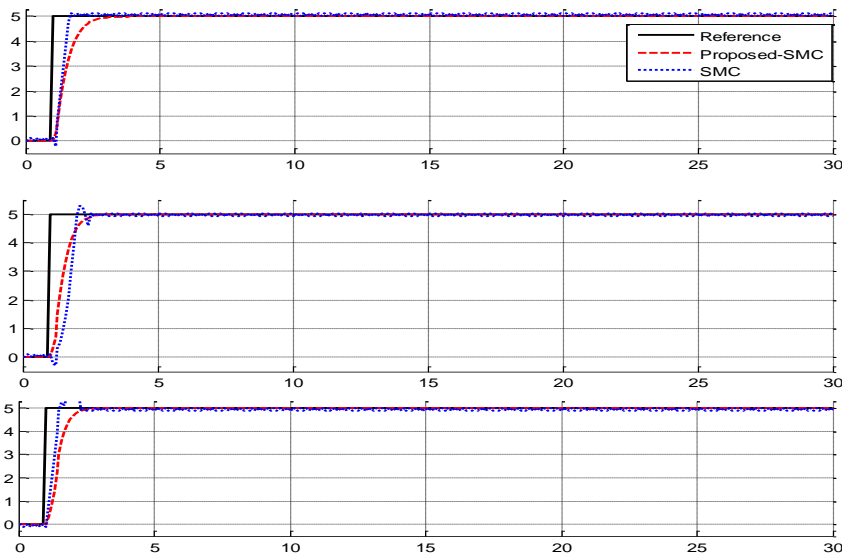

Figure 23. Trajectory Following: SMC and Proposed SMC

Figure 24 shows the disturbance rejection in sliding mode controller and improve sliding mode controller. Regarding to the following Figure, SMC has high frequency oscillation (chattering) in presence of uncertainty that improved SMC eliminate this challenge. However, proposed SMC eliminate the chattering but in uncertainty, it has some challenge (in-stability).
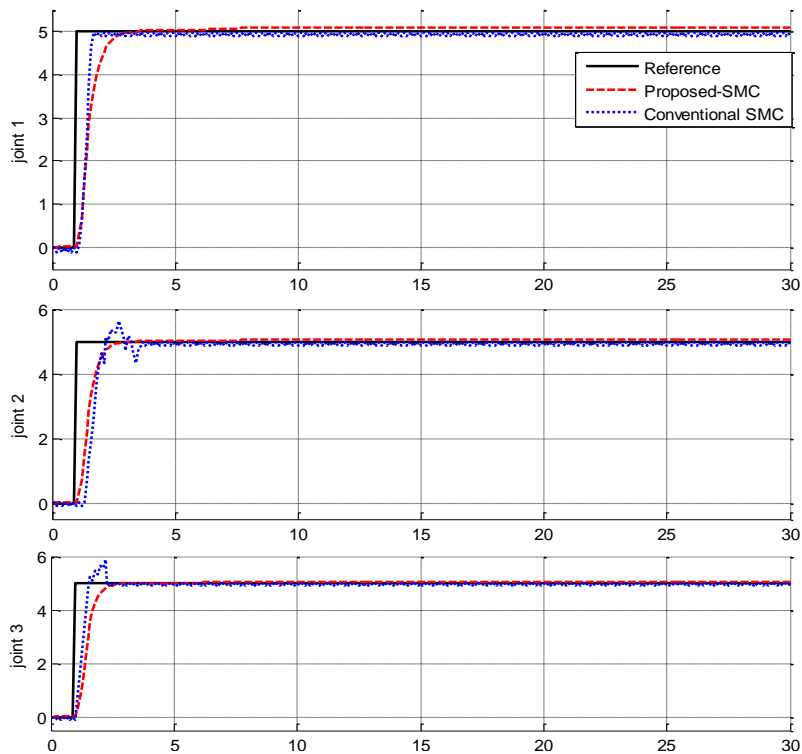
Figure 24. Disturbance Rejection: SMC and Proposed SMC

Timing Report: FPGA-based proposed SMC reduce the process time as well improve stability and flexibility. Figure 25 shows the actual and desired input, and torque performance in transient state. Regarding to this Figure however actual and desired inputs equal to zero but torque performance has fluctuations in first $10\,ns$.

Figure 25. FPGA-Based Controller in Fist 10 ns

Figure 26 indicates the actual and desired position, and torque performance. In this state the desired position is $0\,degrees$ but in the next $50\,ns$ the actual position is $0\,degrees$. Regarding to the following Figure it has about zero degrees error.
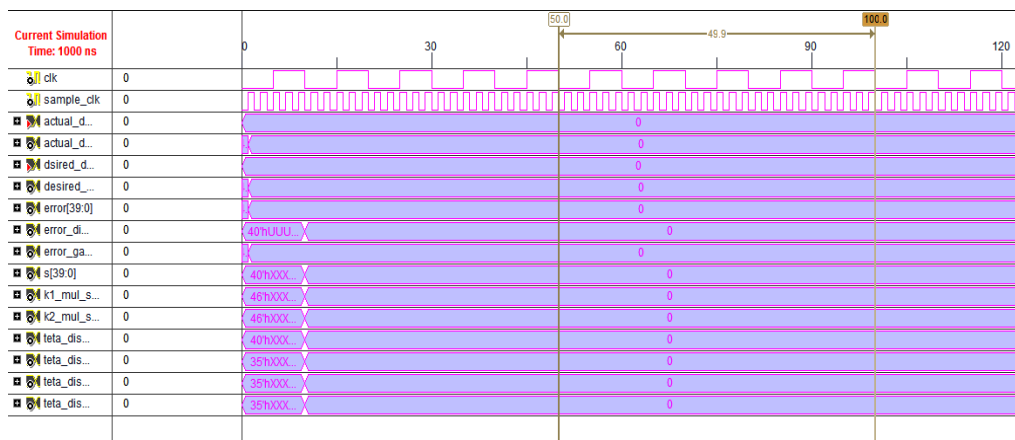
Figure 26. FPGA-Based Controller Result Between 50-100 ns

Regarding to Figure 27, the torque performance between 100 to 130 ns is equal to zero. In this time controller is inactive, this time is the controller's delay. The next $20\,ns$ $(130 - 150\,ns)$ illustrate the desired position is 50 degrees and improvement the actual position from $0\,degrees$ to $43\,degrees$. Regarding to the Figure 27 the error is about $7\,degrees$.
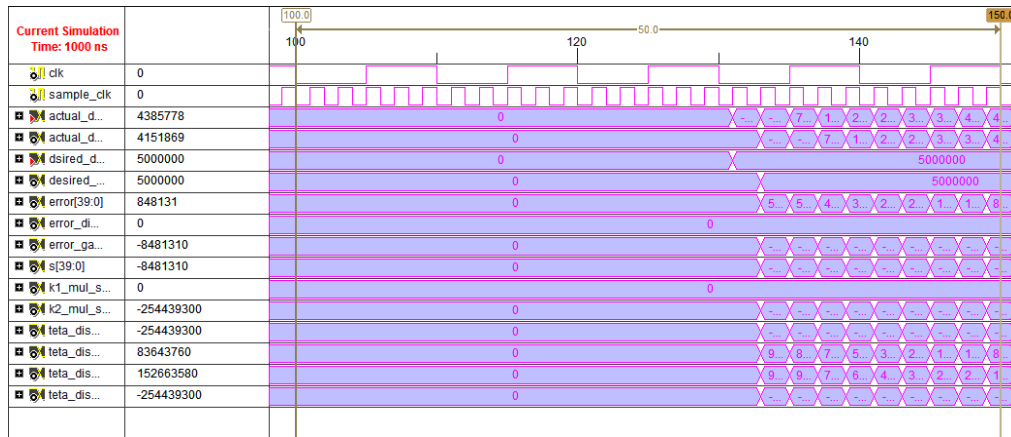
Figure 27. FPGA-Based Controller Result between 100-150 ns

Figure 28 shows the timing report between $(150 - 250\ ns)$. Regarding to the following Figure the error reduce from $7\ degrees$ to $0.1\ degrees$ and the power of torque performance improve from $-254 \frac{N.M}{s}$ to $-0.1 \frac{N.M}{s}$.
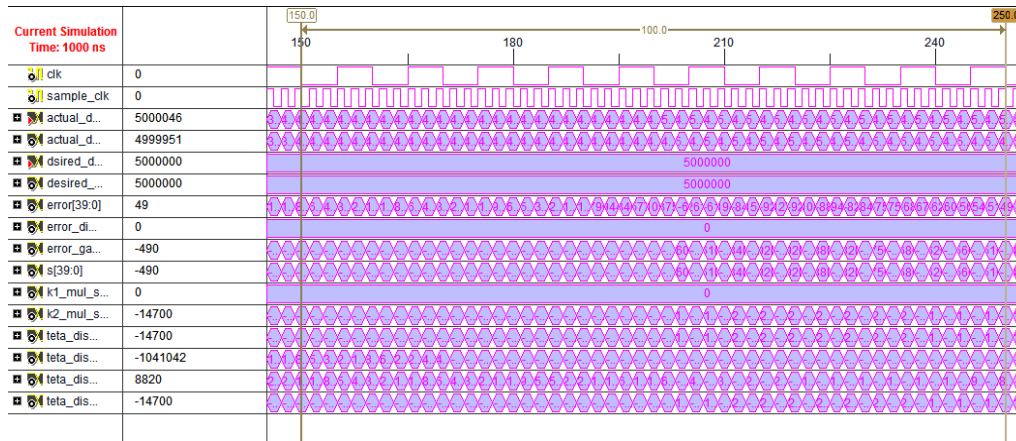

Figure 28. FPGA-Based Controller Result between 150-250 ns

Figure 29 shows the timing report between $degrees$ to $0.1\ degrees$ and the power of torque performance improve from $-254 \frac{N.M}{s}$ to $-0.1 \frac{N.M}{s}$ $(150 - 250\ ns)$. Regarding to the following Figure the error reduce from 7 .
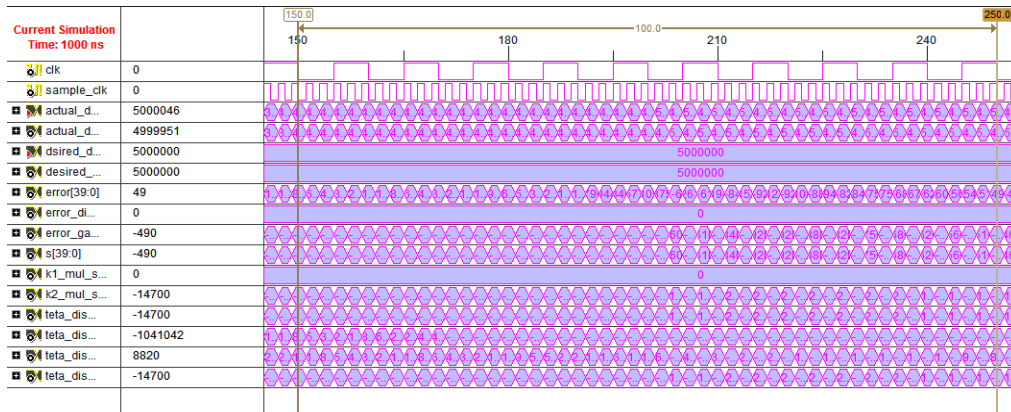

Figure 29. FPGA-Based Controller Result between 150-250 ns

Figure 30 shows the timing report between $(470 - 1000\ ns)$. Regarding to the following Figure the error reduce from $0.1\ degrees$ to $0\ degrees$ and the power of torque performance improve from $-0.1\frac{N.M}{S}$ to $0\ \frac{N.M}{S}$.
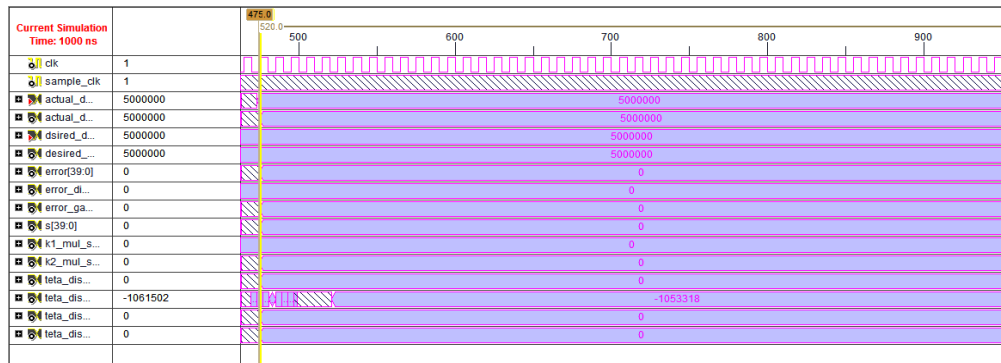

Figure 30. FPGA-Based Controller Result between 470-1000 ns

5. Conclusion

From the design and simulation results of the proposed controller, it can be concluded that; higher execution speed versus small chip size is achieved by designing improved SMC-FPGA based controller with simplified structure. This method improves the speed of system performance and reduces the delay of system's control. As a result, in XILINX group FPGA's, it is observed that; the timing delay constraint is 15.7 ns in that *87.8%* for logic gates and *12.2%* for routes, 46 levels of logic with *1307112* total pats. This design has *4.4 ns* (56.2% logics and 43.8% routes) offsets in two levels of logic circuit design. Regarding to MATLAB test and result, proposed method reduce/eliminate the chattering in certain and uncertain condition.Therefore, the proposed controller will be able to control a wide range of the systems with high sampling rate.

Acknowledgment

References

[1]   B. Armstrong, O. Khatib and J. Burdick, "The explicit dynamic model and inertial parameters of the PUMA 560 arm", IEEE International Conference on Robotica and Automation, **(2002)**, pp. 510-518.

[2]   T. R. Kurfess, Robotics and automation handbook: CRC, **(2005)**.

[3]   B. Siciliano and O. Khatib, Springer handbook of robotics: Springer-Verlag New York Inc, **(2008)**.

[4]   R. Palm, "Sliding mode fuzzy control", IEEE International conference on Fuzzy Systems, **(2002)**, pp. 519-526.

[5]   J. J. E. Slotine, "Sliding controller design for non-linear systems", International Journal of Control, vol. 40, no. 2, **(1984)**, pp. 421-434.

[6]   J. J. Slotine and S. Sastry, "Tracking control of non-linear systems using sliding surfaces, with application to robot manipulators†", International Journal of Control, vol. 38, no. 2, **(1983)**, pp. 465-492.

[7]   R. A. DeCarlo, S. H. Zak and G. P. Matthews, "Variable structure control of nonlinear multivariable systems: a tutorial", Proceedings of the IEEE, vol. 76, no. 3, **(2002)**, pp. 212-232.

[8]   K. D. Young, V. Utkin and U. Ozguner, "A control engineer's guide to sliding mode control", IEEE International Workshop on Variable Structure Systems, **(2002)**, pp. 1-14.

[9]   O. Kaynak, "Guest editorial special section on computationally intelligent methodologies and sliding-mode control", IEEE Transactions on Industrial Electronics, vol. 48, no. 1, **(2001)**, pp. 2-3.

[10] I. Boiko, L. Fridman, A. Pisano and E. Usai, "Analysis of chattering in systems with second-order sliding modes", IEEE Transactions on Automatic Control, vol. 52, no. 11, **(2007)**, pp. 2085-2102.

[11] V. Utkin, "Variable structure systems with sliding modes", IEEE Transactions on Automatic Control, vol. 22, no. 2, **(2002)**, pp. 212-222.

[12] P. I. Corke and B. Armstrong-Helouvry, "A search for consensus among model parameters reported for the PUMA 560 robot", IEEE International Conference on Robotica and Automation, **(1994)**, pp. 1608-1613.

[13] F. Piltan, N. Sulaiman, M. H. Marhaban, A. Nowzary and M. Tohidian, "Design of FPGA-based Sliding Mode Controller for Robot Manipulator", International Journal of Robotic and Automation, vol. 2, no. 3, **(2011)**, pp. 183-204.

[14] F. Piltan, N. Sulaiman, A. Jalali and K. Aslansefat, "Evolutionary Design of Mathematical tunable FPGA Based MIMO Fuzzy Estimator Sliding Mode Based Lyapunov Algorithm: Applied to Robot Manipulator", International Journal of Robotics and Automation, vol. 2, no. 5, **(2011)**, pp. 317-343, 2011.

[15] F. Piltan, I. Nazari, S. Siamak and P. Ferdosali, "Methodology of FPGA-Based Mathematical error-Based Tuning Sliding Mode Controller", International Journal of Control and Automation, vol. 5, no. 1, **(2012)**, pp. 89-118.

Authors

Mahsa Piltan is currently Master Student at Islamic Azad University, Kazeroun branch. Her current research   interests are nonlinear control, artificial control system and design FPGA-based controller.

Abdolwahab Kazerouni is a PhD holder from Wales University of U.K and has taught for almost 25 years at Azad University, Iran and a member of scientific board of Kazeroun Azad University.